

## Old Dominion University ODU Digital Commons

OEAS Faculty Publications

Ocean, Earth & Atmospheric Sciences

2018

# The Biogeochemical Cycling of Iron, Copper, Nickel, Cadmium, Manganese, Cobalt, Lead, and Scandium in a California Current Experimental Study

Travis Mellett

Matthew T. Brown


P. Dreux Chappell  
*Old Dominion University*, [pdchappe@odu.edu](mailto:pdchappe@odu.edu)

Carolyn Duckham

Jessica N. Fitzsimmons

*See next page for additional authors*

Follow this and additional works at: [https://digitalcommons.odu.edu/oeas\\_fac\\_pubs](https://digitalcommons.odu.edu/oeas_fac_pubs)

 Part of the [Biochemistry Commons](#), [Marine Biology Commons](#), and the [Oceanography Commons](#)

### Repository Citation

Mellett, Travis; Brown, Matthew T.; Chappell, P. Dreux; Duckham, Carolyn; Fitzsimmons, Jessica N.; Till, Claire P.; Sherrell, Robert M.; Maldonado, Maria T.; and Buck, Kristen N., "The Biogeochemical Cycling of Iron, Copper, Nickel, Cadmium, Manganese, Cobalt, Lead, and Scandium in a California Current Experimental Study" (2018). *OEAS Faculty Publications*. 256.  
[https://digitalcommons.odu.edu/oeas\\_fac\\_pubs/256](https://digitalcommons.odu.edu/oeas_fac_pubs/256)

### Original Publication Citation

Mellett, T., Brown, M. T., Chappell, P. D., Duckham, C., Fitzsimmons, J. N., Till, C. P., . . . Buck, K. N. (2018). The biogeochemical cycling of iron, copper, nickel, cadmium, manganese, cobalt, lead, and scandium in a California Current experimental study. *Limnology and Oceanography*, 63(1), S425-S447. doi:10.1002/lno.10751

---

**Authors**

Travis Mellett, Matthew T. Brown, P. Dreux Chappell, Carolyn Duckham, Jessica N. Fitzsimmons, Claire P. Till, Robert M. Sherrell, Maria T. Maldonado, and Kristen N. Buck

## The biogeochemical cycling of iron, copper, nickel, cadmium, manganese, cobalt, lead, and scandium in a California Current experimental study

Travis Mellett,<sup>1</sup> Matthew T. Brown,<sup>2</sup> P. Dreux Chappell,<sup>3</sup> Carolyn Duckham,<sup>4</sup>  
Jessica N. Fitzsimmons ,<sup>5,a</sup> Claire P. Till ,<sup>6,b</sup> Robert M. Sherrell,<sup>5</sup> Maria T. Maldonado,<sup>4</sup>  
Kristen N. Buck <sup>1\*</sup>

<sup>1</sup>College of Marine Science, University of South Florida, St. Petersburg, Florida

<sup>2</sup>Natural Sciences Department, Flagler College, St. Augustine, Florida

<sup>3</sup>Department of Ocean, Earth, and Atmospheric Science, Old Dominion University, Norfolk, Virginia

<sup>4</sup>Department of Earth, Ocean, and Atmospheric Sciences, University of British Columbia, Vancouver, British Columbia, Canada

<sup>5</sup>Department of Marine and Coastal Sciences and Department of Earth and Planetary Sciences, Rutgers University, New Brunswick, New Jersey

<sup>6</sup>Ocean Sciences Department, University of California Santa Cruz, Santa Cruz, California

### Abstract

A 3-day shipboard incubation experiment was conducted in the California Current System in July 2014 to investigate the cycling of iron (Fe), copper (Cu), nickel (Ni), cadmium (Cd), manganese (Mn), cobalt (Co), lead (Pb), and scandium (Sc) under a range of light and particle conditions. Filtered (< 0.2 μm) and unfiltered treatments were incubated under the following light conditions: Dark, light (“UV”), and light without the ultraviolet (UV) wavelengths (“noUV”). The experiment was sampled for carbon and Fe uptake rates, dissolved trace metal concentrations (Fe, Cu, Ni, Cd, Mn, Co, Pb, Sc), Fe and Cu speciation, size-fractionated concentrations of Cd and Fe, and diatom community composition from DNA sequencing. Exposure to UV light increased phytoplankton Fe uptake in the first 24 h of the incubation relative to the noUV treatment, suggesting that a fraction of the ambient ligand-bound Fe was photoreactive. Fe-binding organic ligand production was observed in the unfiltered light treatments in association with increasing chlorophyll *a*, and evidence for Cu-binding ligand production in these treatments was also observed. Biological uptake of Cd and Co was observed along with scavenging of dissolved Pb. Manganese appeared to be rapidly oxidized by Mn-oxidizing bacteria with concomitant drawdown of dissolved Ni. Scandium displayed similar trends to Fe, reinforcing the limited observations of the physicochemical similarities between these two elements in seawater. Overall, this study highlights distinct impacts of photochemical processes, scavenging, and biological effects on marine trace metal cycling in an environment characterized by seasonal upwelling.

\*Correspondence: kristenbuck@usf.edu

<sup>a</sup>Present address: Department of Oceanography, Texas A&M University, College Station, Texas

<sup>b</sup>Present address: Chemistry Department, Humboldt State University, Arcata, California

Additional Supporting Information may be found in the online version of this article.

This is an open access article under the terms of the Creative Commons Attribution-NonCommercial-NoDerivs License, which permits use and distribution in any medium, provided the original work is properly cited, the use is non-commercial and no modifications or adaptations are made.

The importance of iron (Fe) as a micronutrient has been established for nearly three decades (Martin and Fitzwater 1988). It is now recognized that Fe limits primary productivity in as much as 40% of the surface ocean and exerts significant influence on carbon cycling in the global ocean (Moore et al. 2004; Boyd et al. 2007; Tagliabue et al. 2017). Although Fe is a major constituent of the Earth’s crust, its physicochemical properties result in low solubility in oxygenated seawater (Liu and Millero 2002). This scarcity in the water column is compounded by a high biological demand for Fe as a cofactor in enzymes that mediate critical biochemical reactions in phytoplankton such as nitrogen fixation and photosynthesis (Sunda 1989; Morel and Price 2003).

In addition to Fe, a suite of bioactive metals including copper (Cu), nickel (Ni), cobalt (Co), cadmium (Cd), and manganese (Mn), among others, have garnered attention for their biological utilization by phytoplankton and have been studied to determine the influence they exert on primary production in the oceans (Sunda 1989; Bruland et al. 1991; Morel and Price 2003; Twining and Baines 2013). For example, Cu is used by Fe-limited diatoms as a cofactor in a high affinity Fe uptake system (Maldonado et al. 2006), and insufficient Cu has been suggested to co-limit phytoplankton growth along with Fe in the subarctic North Pacific (Peers et al. 2005). For some diatom and cyanobacteria taxa, Cd and Co can substitute for Zn in the carbonic anhydrase (CA) enzyme (Price and Morel 1990; Sunda and Huntsman 1995a; Cullen and Sherrell 2005; Xu and Morel 2013), while other taxa require Cd for a distinct Cd-CA (Lane and Morel 2000) and cyanobacteria have an obligate Co requirement (Sunda and Huntsman 1995a; Saito et al. 2002). However, elevated Cu and Cd have also been shown to inhibit phytoplankton growth due to intracellular oxidative stress and antagonism of micronutrient uptake (Brand et al. 1986; Sunda 1989; Sunda and Huntsman 1996). Nickel is required for the acquisition of nitrogen in the form of urea and can be used as a cofactor in a superoxide dismutase to mediate oxidative stress (Price and Morel 1991; Dupont et al. 2010). Many of these enzymes may also have effective (and ineffective) metal substitutes, complicating trace metal biogeochemistry in the surface ocean and our understanding of biological requirements (Saito et al. 2008). Other metals may be useful to tease apart some of these processes, such as scandium (Sc), which has similar physiochemical characteristics to Fe but no apparent biochemical role, and so may be useful in distinguishing between biotic and abiotic mechanisms of Fe cycling (Parker et al. 2016). Similarly, lead (Pb) has no biological function but is especially prone to scavenging via surface absorption to cells and may be passively accumulated through calcium acquisition pathways (Burnett and Patterson 1980; Fisher et al. 1987). Quantifying the cycling of these elements in the ocean requires a deeper understanding of the biogeochemical processes that control their concentrations, speciation and resulting bioavailability in the water column.

In seawater, the dominant chemical forms of these trace metals play a governing role in their bioavailability to planktonic communities. Typically >99% of dissolved Fe and Cu is complexed by a heterogeneous pool of organic ligands (Coale and Bruland 1988; Gledhill and Van Den Berg 1994; Rue and Bruland 1995; Wu and Luther 1995; Moffett and Dupont 2007), and recent studies by the GEOTRACES program indicate that this extensive organic complexation persists throughout the water column and across ocean basins (Buck et al. 2015; Gerringa et al. 2015; Jacquot and Moffett 2015). Changes in ligand concentration appear to be linked to biological activity, as demonstrated in field incubations

(Lohan et al. 2005; Buck et al. 2010; King et al. 2012; Bundy et al. 2016) and large-scale fertilization experiments (Rue and Bruland 1997; Kondo et al. 2008). Most bioactive metals including Zn (Bruland 1989; Ellwood and Van Den Berg 2000; Lohan et al. 2005), Co (Ellwood and Van Den Berg 2001; Saito and Moffett 2001), Cd (Bruland 1992), Mn (Oldham et al. 2015), Pb (Capodaglio et al. 1990), Ni (Nimmo et al. 1989; Saito et al. 2004), and perhaps even Sc (Rogers et al. 1980) form organic complexes to varying degrees in seawater, although they remain far less studied than Fe and Cu.

Marine Fe has been shown to be physically partitioned across a wide size spectrum that includes soluble complexes (< 0.02  $\mu\text{m}$ ) that are “truly dissolved,” colloidal complexes (0.02–0.2  $\mu\text{m}$  in size) that include both inorganic and organically-complexed particles small enough to fall in the operational “dissolved” size fraction (< 0.2  $\mu\text{m}$ ), and larger particulate compounds (> 0.2  $\mu\text{m}$  in size) (Bergquist et al. 2007; Fitzsimmons and Boyle 2014). Additional complexity exists in the biogeochemical cycling of metals that exist in more than one redox state in seawater. Metals such as Fe, Mn, and Cu are subject to reduction by photochemistry in the surface ocean, which changes their chemical properties and thus their solubility and bioavailability to primary producers (Morel and Price 2003). While some bacteria can access organically complexed Fe directly, most phytoplankton preferentially take up inorganic Fe (Morel et al. 2008) and must access ligand-bound Fe using a cell surface reductase to reduce dissolved Fe(III) to Fe(II) (Maldonado and Price 1999; Maldonado and Price 2001; Lis et al. 2015). Laboratory experiments have also shown that some marine derived Fe-bound siderophores degrade in the presence of natural sunlight, resulting in Fe(II) and weaker oxidized organic ligands (Barbeau et al. 2001; Barbeau et al. 2003; Barbeau 2006). Although photochemical degradation is the proposed mechanism for surface minima in organic ligand concentrations, field experiments have reported variable ligand photolability in natural waters (Powell and Wilson-Finelli 2003; Rijkenberg et al. 2006; Bundy et al. 2016).

Field incubation studies are a useful tool for probing the response of natural planktonic communities to changes in micronutrient availability and the processes controlling metal bioavailability. Grow out experiments tracking changes in Fe speciation report strong (i.e.,  $L_1$ -type) ligand production under Fe-limiting conditions, hypothesized to be tied to elevated nitrate: dissolved Fe (dFe) ratios (Buck et al. 2010; King et al. 2012; Bundy et al. 2016). Other incubations have shown that siderophore (also an  $L_1$ -type ligand) bound Fe is bioavailable to planktonic communities (Maldonado and Price 1999; Maldonado and Price 2001), providing a possible mechanism to explain the observed speciation changes. However, it is still unclear if the cause of ligand production in the surface ocean is a direct response to low Fe bioavailability. The organic ligand pool detected using conventional

methods includes strong ligands, which are characteristic of siderophores, but also other weaker ligand classes (i.e.,  $L_2$  to  $L_4$ -type) that likely represent other metal-reactive portions of the dissolved organic carbon pool such as polysaccharides, humic substances, and high molecular weight compounds (Gledhill and Buck 2012). Weak ligand production has also been observed in incubations (Bundy et al. 2016) and attributed to remineralization by bacteria (Boyd et al. 2010), photochemical degradation of stronger  $L_1$  ligands (Barbeau et al. 2001), and viral cell lysis (Poorvin et al. 2011), although the magnitude of each source contribution is still unclear. Indeed, viruses themselves have recently been proposed to constitute a colloidal-sized Fe-binding ligand (Bonnain et al. 2016). The existing observations demonstrate the complexity of trace metal cycling in the surface ocean and the value of experimental studies in natural marine systems.

The processes outlined above are central in dynamic ocean environments like the California Current System (CCS), an eastern boundary upwelling environment characterized by seasonally high productivity and a mosaic of iron limitation (Hutchins et al. 1998; Bruland et al. 2001; Chase et al. 2007). In this study, the role of light and ambient phytoplankton communities on the biogeochemical cycling of Fe and a suite of other bioactive metals was investigated in a 3-d shipboard incubation experiment in the CCS. This experiment applied treatments of different light conditions (with and without UV) in the presence and absence of natural planktonic communities to identify the roles of light-driven abiotic vs. biotic processes on trace metal concentrations and physiochemical speciation. These experiments traced both chemical and biological parameters including Fe and carbon (C) uptake rates, total dissolved trace metal concentrations of Fe, Cu, Ni, Cd, Mn, Co, Pb, and Sc, size-fractionated partitioning of Fe and Cd, dissolved Fe and Cu speciation measurements, macronutrient concentrations, chlorophyll *a* (Chl *a*) measurements, and diatom community structure using genetic markers. The combination of these analyses provides novel insights into feedbacks between trace metal chemistry, the light spectrum, and biological processes in natural waters of the CCS.

## Methods

### Incubation setup

The incubation experiment described here was conducted as part of a collaborative research effort in the CCS led by Professor Ken Bruland on the R/V *Melville* in July 2014. Water for the incubation experiment was collected off the Oregon Coast ( $42^{\circ}39'N$ ,  $124^{\circ}59'W$ , Fig. 1) on 21 July 2014. A trace metal clean surface tow-fish system (Bruland et al. 2005) was used to collect water with a Teflon diaphragm pump from 3 m to 5 m depth while the ship steamed slowly forward ( $\sim 1$ – $2$  knots). Incoming seawater was collected and homogenized in a 210-L high-density polyethylene barrel

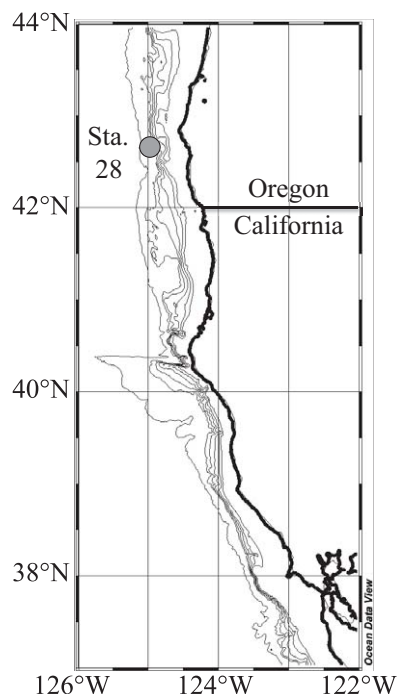


**Fig. 1.** Sampling location for incubation water collection during the July 2014 cruise. The homogenized water used in the experiment was collected near InrBru cruise Sta. 28 off the coast of southern Oregon. The map is overlaid with the 0 m, 200 m, 400 m, 600 m, 800 m, 1000 m, and 2000 m isobaths.

that had been cleaned by soaking with 1% hydrochloric acid (HCl) for several days, rinsed with Milli-Q water ( $\geq 18.2$  M $\Omega$  cm), and rinsed with seawater sample prior to filling. After filling the barrel, the homogenized water was then pumped into 10-L low-density polyethylene (LDPE) Cubitainers<sup>®</sup> (Fisher Scientific 05-719-307) that had been acid-cleaned with 10% trace metal grade HCl and rinsed twice with the experimental seawater prior to filling. An acid-cleaned, seawater-flushed 0.2  $\mu$ m Acropak filter capsule (Pall 500, Fisher Scientific) was used in-line to filter out planktonic communities and particles to fill a subset of the Cubitainers with seawater from the barrel. During filling, each Cubitainer was randomly assigned to a treatment, labeled, and deposited in deck-board incubators, a process which took  $\sim 3.5$  h in total from start to finish. Cubitainers were removed from the incubators at random during each sampling time point. A schematic of the Cubitainer filling process and treatment assignments is shown in Fig. 2.

The deck-board incubators were made of Plexiglas<sup>®</sup>, fitted with hoses to allow continual circulation of surface seawater, and covered with a layer of neutral density screening to achieve  $\sim 50\%$  attenuation of ambient light. Temperature and light intensity measurements were recorded continuously through the experiment using a data logger (HOBO) placed in an adjacent incubator with the same conditions as these incubators. While the HOBO loggers did not measure UV intensity, the National Oceanic and Atmospheric



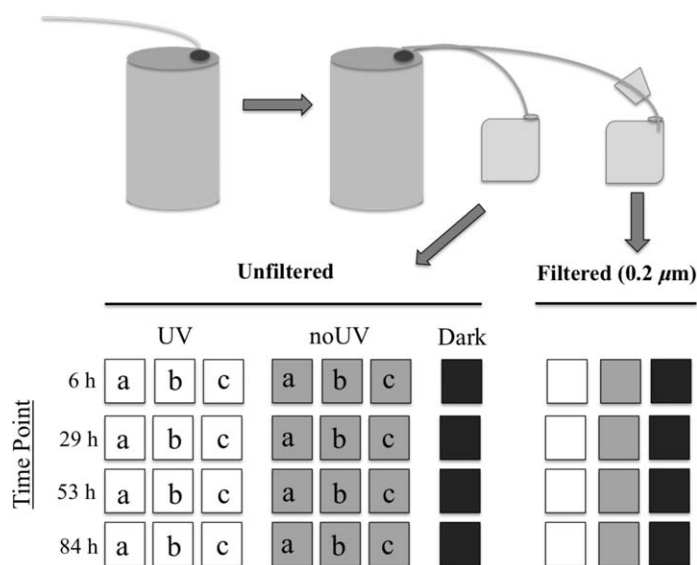


**Fig. 2.** Flow chart depicting the setup of the incubation. A large 210-L plastic barrel was rinsed three times and then filled with surface water collected from a towed sampling fish. Once filled, the water in the barrel was pumped into acid cleaned Cubitainers, either unfiltered or filtered with a 0.2 μm in-line filter. Each Cubitainer was placed in an incubator with one of three light treatments: UV (white), noUV (gray), and Dark (black). UV and noUV treatments contained three replicates (a–c) for each time point.

Administration (NOAA) Climate Prediction Center recorded a “high” (8–10) UV index in July 2014 at monitoring stations from San Francisco, California and Portland, Oregon, the two nearest stations to our study site. There were three different light conditions employed in this experiment (Fig. 2): full spectrum natural light (“UV” treatment, no Plexiglas® cover on the incubator), the same full spectrum light but without the UV wavelengths (“noUV” treatment, with a UV-filtering Plexiglas® cover on the incubator), and dark (“Dark” treatment, in the same incubator in a heavy duty black plastic trash bag). The Cubitainers themselves allowed 80% transmittance of the light spectrum but reduced the UV (< 400 nm) transmittance to 60% for the light treatments; the addition of the Plexiglas®, used for the noUV treatment, further reduced the UV transmittance to 0% (Supporting Information Fig. S1). For each of the light treatments, a subset of Cubitainers containing 0.2 μm-filtered seawater were filled as controls for the unfiltered treatments in order to facilitate distinction between bottle effects and particle influences in the experiment.

**Incubation sampling**

The experimental sampling design (Fig. 2) used was intended to minimize sample handling and the associated contamination risks by eliminating repeat-sampling from a single Cubitainer at various time points (Lohan et al. 2005). Instead, an entire Cubitainer was sampled at each time point and it was assumed that all Cubitainers began with identical

conditions present in the initial sample and that replicates (a, b, and c in Fig. 2) were representative of each other within treatments. The advantage of this sampling approach was that it minimized the potential for contamination of the Cubitainer during sampling, which would have complicated interpretation of results from later time points from the same container. A drawback of this approach was that it limited assessment of Cubitainer-specific effects (contamination, variable light exposure, differential grazing, etc.) on the parameters measured, likely resulting in higher intra-treatment variability, though these effects were expected to be negligible compared to inter-treatment variability.

The incubation was started at 13:00 h local time and a random Cubitainer from each treatment was sampled at 6 h, 29 h, 53 h, and 84 h. For the unfiltered light treatments (both UV and noUV), three replicates (Cubitainers a, b, c) were sampled for each time point. For the Dark treatments and all of the filtered treatments, only one Cubitainer was sampled at each time point (Fig. 2). Note that the notation for replicates (a, b, c) was assigned at random by the order sampled.

**Total dissolved trace metals (Fe, Cu, Ni, Cd, Mn, Co, Pb, and Sc)**

Samples collected for dissolved trace metals were filtered through acid-cleaned 0.2 μm polycarbonate track-etched (PCTE; Whatman) filters on an all-Teflon filtration rig (Savillex) under ~ 0.5 atm pressure into acid-cleaned and sample-rinsed 125 mL LDPE (Nalgene) bottles. Filtrate was acidified at sea with the equivalent of 4 mL 6 M quartz-distilled HCl per liter of seawater (to 0.024 M HCl, pH ~ 1.8) and left acidified for ~ 8 months prior to analysis (Johnson et al. 2007). Dissolved metals were analyzed at the University of California Santa Cruz with an adaptation of Biller and Bruland (2012) as described in Parker et al. (2016). Briefly, this method involved UV irradiation of the seawater samples for 120 min to ensure recovery of the organic-bound Cu and Co, followed by pre-concentration of the metals of interest on Nobias PA1® chelating resin at pH 6.0. Metals were eluted from the column with 1 N quartz-distilled nitric acid (HNO<sub>3</sub>), and the eluent was analyzed on an Element XR inductively coupled plasma mass spectrometer (ICP-MS) using standard curves and standard additions for quantification of concentrations and percent recoveries. The accuracy of metal concentrations measured using this method was assessed by reference to consensus values of seawater reference materials (Table 1).

**Size-fractionated Cd and Fe**

Dissolved (< 0.2 μm) metals were separated into soluble (< 0.02 μm) and colloidal (0.02–0.2 μm) size fractions by passing seawater through acid-cleaned, 47 mm Anodisc (0.02 μm) membrane filters on an all-Teflon filtration rig (Savillex) under ~ 0.5 atm of pressure (Fitzsimmons and Boyle 2014). Ultrafiltrate containing the soluble metal fraction was

**Table 1.** Measured and consensus values for seawater reference samples collected using the two analytical methods in this study: the OSC method of Parker et al. (2016) (for  $< 0.2 \mu\text{m}$  dissolved samples) and the SeaFAST Isotope Dilution method modified from Lagerström et al. (2013) (for  $< 0.02 \mu\text{m}$  soluble samples). Consensus values are valid as of May 2013 and are taken from <http://www.geotraces.org/sic/intercalibrate-a-lab/standards-and-reference-materials>.

Metal ( $\text{nmol kg}^{-1}$ )	SAFe S			SAFe D2		
	OSC	SeaFAST	Consensus	OSC	SeaFAST	Consensus
Cd*	$1.0 \pm 0.2$ ( $n=17$ )	$1.2 \pm 2.3$ ( $n=25$ )	$1.1 \pm 0.3$	$974 \pm 25$ ( $n=23$ )	$1002 \pm 13$ ( $n=25$ )	$986 \pm 23$
Fe	$0.095 \pm 0.014$ ( $n=12$ )	$0.097 \pm 0.024$ ( $n=25$ )	$0.093 \pm 0.008$	$0.98 \pm 0.19$ ( $n=19$ )	$0.938 \pm 0.057$ ( $n=25$ )	$0.933 \pm 0.023$
Mn	$0.81 \pm 0.07$ ( $n=23$ )	—	$0.79 \pm 0.06$	$0.37 \pm 0.04$ ( $n=20$ )	—	$0.35 \pm 0.05$
Ni	$2.36 \pm 0.15$ ( $n=24$ )	—	$2.28 \pm 0.09$	$8.48 \pm 0.47$ ( $n=23$ )	—	$8.63 \pm 0.25$
Cu	$0.51 \pm 0.04$ ( $n=24$ )	—	$0.52 \pm 0.05$	$2.19 \pm 0.08$ ( $n=23$ )	—	$2.28 \pm 0.15$
Co*	$5.3 \pm 1.1$ ( $n=22$ )	—	$4.8 \pm 1.2$	$46.6 \pm 3.6$ ( $n=23$ )	—	$45.7 \pm 2.9$
Pb*	$48.5 \pm 2.2$ ( $n=27$ )	—	$48.0 \pm 2.2$	$26.7 \pm 1.1$ ( $n=23$ )	—	$27.7 \pm 1.5$
Sc*	$1.00 \pm 0.30$ ( $n=27$ )	—	—	$6.62 \pm 0.39$ ( $n=23$ )	—	—

\*Values are presented in  $\text{pmol kg}^{-1}$ .

collected into acid-cleaned 60 mL LDPE bottles after a single bottle rinse and then acidified with the equivalent of 4 mL of 6 M quartz-distilled HCl per liter of seawater to achieve 0.024 M HCl in the samples (Johnson et al. 2007).

Approximately a year after acidification, soluble Fe and Cd were analyzed after preconcentration using an offline adaptation of the SeaFAST pico metal extraction system onto Nobias PA1 chelating resin at pH 6.5 (Lagerström et al. 2013). Quantification was accomplished by isotope dilution for Fe and Cd, which were eluted in 10% v/v Optima  $\text{HNO}_3$ . The eluent was analyzed on a Thermo Fisher Element 1 ICP-MS at the Rutgers Inorganic Analytical Laboratory in low (Cd) and medium (Fe) resolution. Colloidal Fe and Cd were calculated by subtracting the soluble concentrations from the dissolved concentrations.

The accuracy of metal concentrations measured using this method were assessed and compared to the offline standard curve (OSC) analytical method used in this study by reference to consensus values of seawater reference materials (Table 1) and by intercalibration with field samples (Supporting Information Fig. S2). While the two methods generally agreed with consensus values for both elements, dFe measurements of SaFe D2 from the OSC method gave values  $\sim 5\%$  higher than the consensus. A separate intercalibration of  $0.2 \mu\text{m}$  filtered seawater samples collected at Sta. 9 of this cruise ( $39^\circ 23' \text{N}$ ,  $124^\circ 40' \text{W}$ ) using GO-Flo bottles suspended on a Kevlar<sup>TM</sup> wire (Bruland et al. 1979) showed that dFe and dCd compared well for these samples across the two dissolved metal analytical methods (Supporting Information Fig. S2).

#### Dissolved Cu and Fe speciation

Filtered ( $< 0.2 \mu\text{m}$ , PCTE, see dissolved trace metals section above) samples were collected for dissolved Fe-binding and Cu-binding organic ligand analyses in 500 mL fluorinated

polyethylene bottles (Buck et al. 2012). These sample bottles were cleaned by soaking in a soap bath for at least 1 week, and then placed in a 25% trace metal grade HCl bath for at least a month. After 1 month, bottles were removed and rinsed 3–5 times with Milli-Q water before being stored filled with Milli-Q until use. Bottles were rinsed again with filtered seawater prior to filling with sample. Samples were then either refrigerated and analyzed within hours of sampling or frozen ( $-20^\circ\text{C}$ ) for analysis back in the laboratory.

Cu- and Fe-binding organic ligands were measured using competitive ligand exchange adsorptive cathodic stripping voltammetry (CLE-AdCSV). The competitive ligand salicylaldehyde (SA) was used to compete with natural ligands (Campos and Van Den Berg 1994; Rue and Bruland 1995; Buck and Bruland 2005; Buck et al. 2007; Buck et al. 2015) and measurements were made on a BioAnalytical Systems (BASi) controlled growth mercury electrode interfaced with an Epsilon 2 analyzer (BASi). For Cu titrations, 15 additions from +0 nM to 25 nM Cu were used and for Fe, 15 additions from +0 nM to 10 nM Fe were used in separate vials. Final SA concentrations of  $2.5 \mu\text{M}$  and  $25 \mu\text{M}$  were used for Cu and Fe speciation measurements, respectively (Buck et al. 2012). Metal additions were allowed to equilibrate for at least 2 h (and often overnight), and SA additions were equilibrated at least another 1 h before analysis (Buck et al. 2012; Abualhaija and Van Den Berg 2014). Deposition times of 300 s and 90 s were used for Cu and Fe speciation, respectively, and Cu samples were purged with  $\text{N}_2$  gas for 180 s prior to analysis (Campos and Van Den Berg 1994; Buck and Bruland 2005; Jacquot and Moffett 2015).

Titration data for both metals was interpreted using ProMCC software (Omanović et al. 2015; Pižeta et al. 2015), which fits the data using multiple regression models. The software was able to fit all titrations for at least one ligand class and several titrations for two ligand classes. Due to the

difficulty in resolving two ligand classes, particularly for Cu, we chose to model Cu-binding ligands using a single ligand class. This speciation information was then used to calculate the free  $[\text{Cu}^{2+}]$  using a quadratic derivation and the assumed side-reaction coefficient of 200 for weaker ligands (Moffett and Dupont 2007). Values presented for  $\alpha'_{\text{FeL}}$  and  $\alpha'_{\text{CuL}}$  were calculated as  $\sum_{i=1} eL_i * K_{\text{FeL}_i, \text{Fe}'}^{\text{cond}}$  and  $eL * K_{\text{CuL}, \text{Cu}^{2+}}^{\text{cond}}$ , respectively. For Fe-binding ligand results, ligand classes were assigned by measured conditional stability constants as described by Gledhill and Buck (2012). Detection limits additional details of this approach are provided in Buck et al. (2015).

### Iron and carbon uptake

Fe and C uptake rates were measured twice over a 7-h period on day 1 of the incubation using 1-L Cubitainers (Fisher Scientific 14-375-115B) with triplicates for each light treatment, henceforth termed “short-term Fe uptake.” The radiotracer  $^{55}\text{Fe}$  was added at low concentrations (0.2 nM; specific activity 10.18 mCi  $\text{mg}^{-1}$  Fe) in order to prevent changes to in situ Fe speciation, but allow equilibrium with ambient organic ligands. To prevent the loss of  $^{55}\text{Fe}$  to the walls of the Cubitainers,  $^{55}\text{Fe}$  was first bound to 0.3 nM EDTA, and then equilibrated for 2 h with 50–100 mL of in situ seawater to allow complexation with ambient organic ligands. This was confirmed by organic complexation measurements of cold (nonradioactive) Fe-EDTA additions, which found the addition to behave as an inorganic Fe addition, binding to the excess  $L_1$  type ligands present in the sample over the titration equilibration. C uptake rates were measured concomitantly, by adding 20  $\mu\text{Ci L}^{-1}$  of the radiotracer  $^{14}\text{C}$  (as  $\text{NaH}^{14}\text{CO}_3$ ; specific activity 52.5 mCi  $\text{mmol}^{-1}$ ).

Fe uptake rates were also measured separately on day 1 (~24 h), day 2 (45–50 h), and day 3 (75–80 h), henceforth called “long-term Fe-uptake” measurements. For these measurements, 0.2 nM  $^{55}\text{Fe}$  was added at the start of the experiment (as described above) to separate 10-L Cubitainers in the UV and noUV treatments (in triplicate). These Cubitainers were resampled twice per day over the course of the experiment (days 1 and 3). This experiment allowed  $^{55}\text{Fe}$  to equilibrate with the in situ Fe and organic ligands and be exposed to the abiotic and biotic processes in the Cubitainers over the full time course of the experiment. The samples were collected by sequentially filtering onto 47 mm polycarbonate filters (0.2  $\mu\text{m}$ , 1  $\mu\text{m}$ , and 5  $\mu\text{m}$ ) that were separated by drain disks. The Fe and C uptake data were normalized to phytoplankton biomass using Chl *a* concentrations from each replicate. Data were collected in triplicate, allowing a statistical comparison of the effect of different light treatments on Fe and C uptake rates using an analysis of variance (ANOVA). Detailed descriptions of the measurement methodology can be found in previous work (Maldonado and Price 1999).

When the concentrations of Fe are mimicked in a culture vs. in a short-term Fe uptake experiments, the calculated steady-state Fe uptake rate should be identical to the short-

term Fe rates. We report both short-term Fe uptake rates and what we called long-term Fe uptake rates, which would be equivalent to steady-state Fe uptake rate in culture.

### Diatom community composition

DNA was collected from the same 47 mm diameter 0.2  $\mu\text{m}$  pore size PCTE filters used in dissolved metal filtration, which were placed in 2 mL cryotubes filled with Qiagen® RLT Plus Buffer (Qiagen, Germany), frozen in liquid nitrogen, and stored at  $-80^\circ\text{C}$  until processing. Filters were extracted using the Qiagen® Allprep RNA/DNA co-extraction with an additional bead-beating step and homogenation using the QIAshredder column (Qiagen, Germany). The V4 region of the 18S rDNA was amplified by polymerase chain reaction (PCR) in triplicate using primers designed to target diatoms (Zimmermann et al. 2011) that were modified for Illumina sequencing and sequenced by the Rhode Island Genomics & Sequencing Center at the University of Rhode Island on the Illumina MiSeq sequencer using the  $2 \times 250$  bp sequencing kit. Additional details on the molecular methods employed in this study are provided in the accompanying Supporting Information.

### Chlorophyll and macronutrients

For size-fractionated Chl *a*, samples were filtered onto 5  $\mu\text{m}$ , 1  $\mu\text{m}$ , and 0.2  $\mu\text{m}$  PCTE filters, separated by drain-disks, and extracted in methanol overnight at  $4^\circ\text{C}$ . The methanol extracts were then measured by fluorometry for Chl *a* determination (Holm-Hansen and Riemann 1978). Total Chl *a* was determined to be the summation of all size fractions measured. Nitrate + nitrite, phosphate, and silicate were determined in filtered ( $< 0.2 \mu\text{m}$ , see trace metal sampling below) samples using a Lachat QuickChem 800 Flow Injection Analysis System following standard spectrophotometric methods (Parsons 1984).

## Results

### Initial conditions

This incubation experiment was conducted in July 2014 off the coast of southern Oregon (Fig. 1). The seawater used for the incubation experiment was pumped from 3 m to 5 m depth via a towed “fish” (Bruland et al. 2005), and was characterized by an initial temperature of  $10.4^\circ\text{C}$  and a salinity of 33.4. The initial temperature of the incubator was  $12.8^\circ\text{C}$ . Total initial Chl *a* concentrations were low ( $1.19 \mu\text{g L}^{-1}$ ) in the homogenized waters, and nearly half of the initial biomass was detected in the 1–5  $\mu\text{m}$  size fraction with the other half roughly split between the larger ( $> 5 \mu\text{m}$ ) and smaller (0.2–1  $\mu\text{m}$ ) size fractions (Figs. 3, 4; Supporting Information; Table S1). Initial concentrations of the macronutrients nitrate + nitrite (“nitrate”), phosphate, and silicate were 17.0  $\mu\text{M}$ , 1.52  $\mu\text{M}$ , and 17.8  $\mu\text{M}$ , respectively (Fig. 3; Table S1). Initial concentrations of the dissolved metals Fe, Cu, Ni, Cd, Mn, Co, Pb, and Sc were 0.90 nM, 1.46 nM, 5.23 nM, 570 pM,



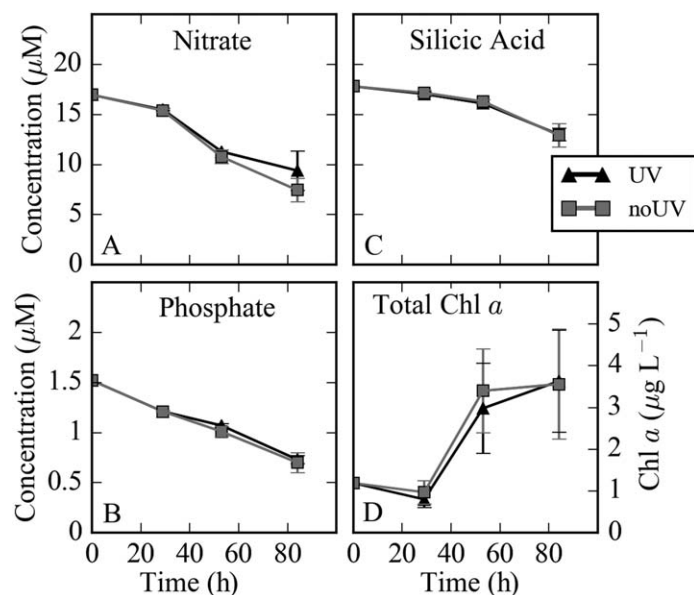


**Fig. 3.** Macronutrient concentrations ( $\mu\text{M}$ ) and total Chl *a* ( $\mu\text{g L}^{-1}$ ) measurements for UV (black triangles) and noUV (gray squares) treatments in the 84-h incubation. (A) nitrate + nitrite (nitrate), (B) phosphate, (C) silicic acid, (D) total Chl *a* concentrations. Error bars represent the standard deviation of the replicate measurements. Total Chl *a* represents the summation of all three ( $> 5 \mu\text{m}$ ,  $1\text{--}5 \mu\text{m}$ , and  $0.2\text{--}1 \mu\text{m}$ ) size fractions measured.

3.72 nM, 157 pM, 32.9 pM, and 2.8 pM, respectively (Fig. 5; Table S2). The colloidal fractions of Fe and Cd at the start of the incubation were 62% and 7%, respectively, of the total dissolved concentrations (Fig. 6). Initial concentrations of Fe-binding organic ligands were 1.38 nM of a stronger L<sub>1</sub>-class ligand ( $\log K_{\text{FeL,Fe}'}^{\text{cond}} > 12$ ) with  $\log K_{\text{FeL,Fe}'}^{\text{cond}} = 12.98$  nM and 1.70 nM of a weaker L<sub>2</sub>-class ligand ( $\log K_{\text{FeL,Fe}'}^{\text{cond}} = 11.05$ ), resulting in a total Fe-binding organic ligand concentration of 3.08 nM with 2.18 nM of ligands in excess of dissolved Fe concentrations (Fig. 7; Table S3). Dissolved Cu-binding organic ligands were not analyzed for the initial conditions, but values from  $\sim 40$  m depth from nearby Sta. 28 were 3 nM with  $\log K_{\text{CuL,Cu}^{2+}}^{\text{cond}} = 13.87$  (Caprara et al. unpubl.).

### Dark treatments

A combination of filtered and unfiltered Dark treatments was employed to evaluate potential bottle effects of the Cubitainers over time (Dark<sub>filtered</sub>) and the relative influence of remineralization and scavenging processes (Dark) on results in the absence of light. There was only one Cubitainer for each Dark time point, and results from these treatments were thus limited to a single replicate. In the Dark, total Chl *a* declined by  $\sim 40\%$  over the 84 h incubation (Fig. 3). Chl *a* samples were not collected from any of the filtered treatments since particles were filtered out of these treatments prior to incubation. Final nitrate and silicate concentrations were within 2% of initial concentrations in both

Dark treatments, while phosphate concentrations in the Dark and Dark<sub>filtered</sub> bottles were lower in final time points by 12.5% and 10%, respectively (Fig. 3).

Dissolved concentrations of Cd, Cu, Co, and Pb were nearly identical between initial and final time points in both the Dark and Dark<sub>filtered</sub> treatments and dCd concentrations remained between 96% and 99% as soluble form for the entirety of the incubation in these treatments (Figs. 5, 6). In the Dark<sub>filtered</sub> treatment dNi and dMn also remained relatively constant, while in the Dark dNi and dMn concentrations declined over the course of the incubation, by 29% and 65%, respectively (Fig. 5D,G). Dissolved Fe and dSc concentrations in both Dark and Dark<sub>filtered</sub> treatments declined and remained below initial concentrations for the first 53 h of the incubation. Between the last two time points of both treatments, however, dFe and dSc concentrations increased to concentrations at or above initial conditions in the 84 h sample (Fig. 5P,S). Final dFe concentrations in the Dark<sub>filtered</sub> and Dark treatments were 0.91 nM and 2.0 nM, respectively, with the dFe increase detected almost entirely in the colloidal fraction (Fig. 6G–L). Final concentrations of dSc for Dark<sub>filtered</sub> and Dark treatments were 7.6 pM and 4.8 pM, respectively (vs. 2.8 pM initially); the colloidal fraction of this element was not measured. The dissolved concentrations of Cd, Cu, Co, and Pb also appeared to increase slightly between these last two time points in the Dark treatment only, though the absence of replicate samples precludes assessment of significance in these measurements.

Dissolved Cu- and Fe-binding organic ligands decreased over the course of the incubation in both the Dark<sub>filtered</sub> and Dark treatment bottles. Total Fe-binding ligand concentrations decreased from  $3.08 \pm 0.29$  nM initially to final concentrations of  $2.18 \pm 0.22$  nM in Dark<sub>filtered</sub> and  $2.55 \pm 0.09$  nM in Dark (Fig. 7). For Cu, ligand concentrations decreased from  $2.72 \pm 0.11$  nM to  $2.23 \pm 0.11$  nM between the 6 h and 84 h time points in the Dark<sub>filtered</sub>, and from  $3.84 \pm 0.29$  nM to  $2.59 \pm 0.17$  nM over the same period in the Dark (Fig. 7; Supporting Information Table S4). Excess ligand concentrations ( $[\text{eL}_{\text{Cu}}] = [\text{L}_T] - [\text{dCu}]$ ,  $[\text{eL}_{\text{Fe}}] = [\text{L}_T] - [\text{dFe}]$ ) generally followed the trends of total ligand concentrations between individual time points in the Dark and Dark<sub>filtered</sub> treatments for both metals (Fig. 7A,D).

### Abiotic (filtered) light treatments

Filtered ( $< 0.2 \mu\text{m}$ ) light treatments (both UV<sub>filtered</sub> and noUV<sub>filtered</sub>) were employed to evaluate whether photochemical reactions impact bottle effects. These treatments displayed similar results to those observed in the Dark<sub>filtered</sub> treatment; light alone did not have a pronounced effect on macronutrient concentrations, dissolved metal concentrations, or metal speciation (Fig. 5). As with the Dark treatments, these abiotic light treatments were also limited to a single Cubitainer (i.e., a single replicate) and so while trends are noted, significance of these trends could not be assessed. Dissolved Cu, Ni, Cd,

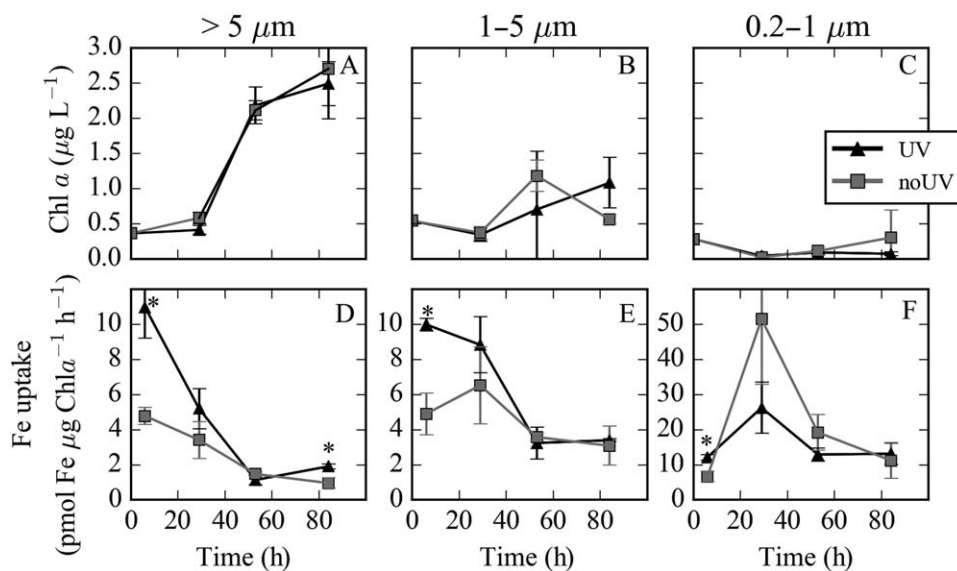


**Fig. 4.** Size fractionated Chl *a* ( $\mu\text{g Chl } a \text{ L}^{-1}$ ) and iron (Fe) uptake measurements ( $\text{pmol Fe } \mu\text{g Chl } a^{-1} \text{ h}^{-1}$ ) for UV (black triangles) and noUV (gray squares). Chl *a* is presented for three different size fractions: (A)  $> 5 \mu\text{m}$ , (B)  $1-5 \mu\text{m}$ , and (C)  $0.2-1 \mu\text{m}$  over the 84 h incubation. In the lower panels, the combined short-term ( $< 7 \text{ h}$ ) and long-term ( $\sim 24 \text{ h}$ ,  $47 \text{ h}$ , and  $78 \text{ h}$ ) Fe uptake rates are displayed for the same size fractions (D)  $> 5 \mu\text{m}$ , (E)  $1-5 \mu\text{m}$ , and (F)  $0.2-1 \mu\text{m}$  over the same period. Error bars represent the standard error of the averages calculated triplicate measurements. \* results that are significantly (ANOVA,  $p < 0.05$ ) different between UV and noUV measurements.

Mn, Co, and Pb presented minimal concentration changes through the incubation in all of the filtered treatments, with no discernible difference between the  $\text{Dark}_{\text{filtered}}$ ,  $\text{UV}_{\text{filtered}}$ , and  $\text{noUV}_{\text{filtered}}$  (Fig. 5). Dissolved Fe and Sc patterns were similar in the  $\text{UV}_{\text{filtered}}$  and  $\text{noUV}_{\text{filtered}}$  to that observed in the  $\text{Dark}_{\text{filtered}}$ , with dFe and dSc concentrations decreasing after the initial time points and increasing dramatically between the last two time points (Fig. 5).

The total concentration of Fe-binding organic ligands remained relatively constant in the presence of UV light, but they transitioned toward a weaker  $L_2$  class ( $\log K_{\text{FeL,Fe}}^{\text{cond}}$  between 11.25 and 11.9) with the exception of the final sample, in which a large concentration of  $L_1$  ligands was detected concomitantly with the increase in colloidal Fe (Figs. 6C,D, 7B,C). In the noUV treatment,  $L_1$  concentrations declined slightly from 1.2 nM to 0.8 nM for the first 53 h of the incubation, before increasing twofold in the final time point sample (Fig. 6B,C). Organic Cu-binding ligands in the  $\text{UV}_{\text{filtered}}$  treatment declined by 23% between the 6 h and 84 h samples of the incubation with  $\log K_{\text{CuL,Cu}^{2+}}^{\text{cond}}$  values ranging between 13.5 and 14. In the  $\text{noUV}_{\text{filtered}}$  Cu-binding ligand concentrations declined slightly less, by  $\sim 15\%$ , over the same interval with  $\log K_{\text{CuL,Cu}^{2+}}^{\text{cond}}$  values between 13.3 and 14 (Fig. 7E,F).

#### Unfiltered light treatments

The unfiltered light treatments (UV and noUV), as expected, were the only treatments that exhibited measurable phytoplankton growth during the incubation. After an initial lag time of  $\sim 29 \text{ h}$ , total Chl *a* concentrations increased nearly threefold by the 84 h time point in the UV and noUV

treatments (Fig. 3). The majority of this increase was in the largest size fraction ( $> 5 \mu\text{m}$ ; Fig. 4), and by the end of the experiment, the largest size fraction comprised 76–80% of the total Chl *a* (Fig. 4). The biological response resulted in very similar nitrate drawdowns in both of the light treatments during the incubation, by 50% and 55% in UV and noUV, respectively (Fig. 3).

The final sequence data used in the diatom community composition analysis has been submitted to the NCBI Sequence Read Archive with the Bioproject ID PRJNA379150. Bray-Curtis dissimilarity data showed that in both UV and noUV treatments there was very little change in the overall diatom community composition between the 29 h and 53 h sampling times, but a major shift in the community composition between the 53 h and 84 h samples (Fig. 8). Grouping the data at the genus level and examining the top 10 genera of representative samples from each cluster revealed a shift in the UV and noUV treatments between the 53 h and 84 h samplings from a diatom community dominated by *Thalassiosira* spp. to one dominated by *Pseudo-nitzschia* spp. (Fig. 9).

Short-term Fe uptake rates during the first 8 h of the experiment were approximately twofold faster (ANOVA,  $p < 0.05$ ) in the UV compared to the noUV. This trend was observed in all three-size fractions (Table 2; Fig. 4D–F). The effect of UV on Fe-uptake was most pronounced for the largest ( $> 5 \mu\text{m}$ ) size fraction and least pronounced in the smallest phytoplankton ( $0.2-1 \mu\text{m}$ ; Table 2; Fig. 4). In contrast to Fe uptake, the rates of short-term C uptake were not statistically significant in the two light treatments (Table 2).

After 29 h, long-term Fe uptake measurements treatments with UV light were still higher than those without UV light for the 1–5 μm and the > 5 μm phytoplankton size fractions,

although these differences were not statistically significant (Supporting Information Table S5; Fig. 4). In contrast, the rates of Fe uptake after 29 h in the smallest size fraction (0.2–1 μm) were faster in the noUV treatment, which were ~ 10-fold faster than the short-term Fe uptake rates (Tables 2, S5). After 29 h, Chl *a* increased in all size fractions such that Fe uptake rates normalized to Chl *a* biomass correspondingly decreased (Fig. 4). At the 53 h sampling time point, the rates of Fe uptake were identical for both light treatments, regardless of size fraction. At the 84 h time point, Fe uptake rates in the largest size fraction (> 5 μm) were significantly faster in UV (ANOVA,  $p < 0.05$ ) relative to the noUV treatment (Fig. 4D).

With the exception of Cu, dissolved metal concentrations decreased over the course of the incubation in both UV and noUV (Fig. 5). In the case of dissolved Cd, Ni, Co, Pb, and Mn, concentration decreases were largest between the 53 h and 84 h time points ( $t$ -test,  $p < 0.05$ ) relative to the 6 h measurement (Fig. 5). Soluble Cd concentrations tracked dCd concentrations over the incubation (Fig. 6A–D). Dissolved Fe and Sc, however, displayed either no change in concentrations between these last two time points (e.g., noUV, Fig. 5Q,T) or an increase in concentration (e.g., UV, Fig. 5O,R). Soluble Fe concentrations remained low through the end of the incubation, indicating that any increases in dFe were in the colloidal size fraction (Fig. 5R,U). Although there was substantial variability in replicate measurements, dCu was the only metal that did not show clear increases or decreases over the course of the incubation in these treatments (Fig. 5K,L).

Total dissolved Fe-binding organic ligand concentrations and excess Fe-binding ligand concentrations increased in the UV and noUV treatments between the 29 h and 53 h time points, concomitant with the Chl *a* increases observed (Fig. 7). In the noUV treatment, ligand concentrations and excess ligand concentrations declined between the 53 h and 84 h time points, with final concentrations of both parameters similar to the concentration in the noUV<sub>filtered</sub> at this time point, although the data represents only one replicate measurement due to sample volume constraints. In the UV, however, total and excess Fe-binding ligand concentrations

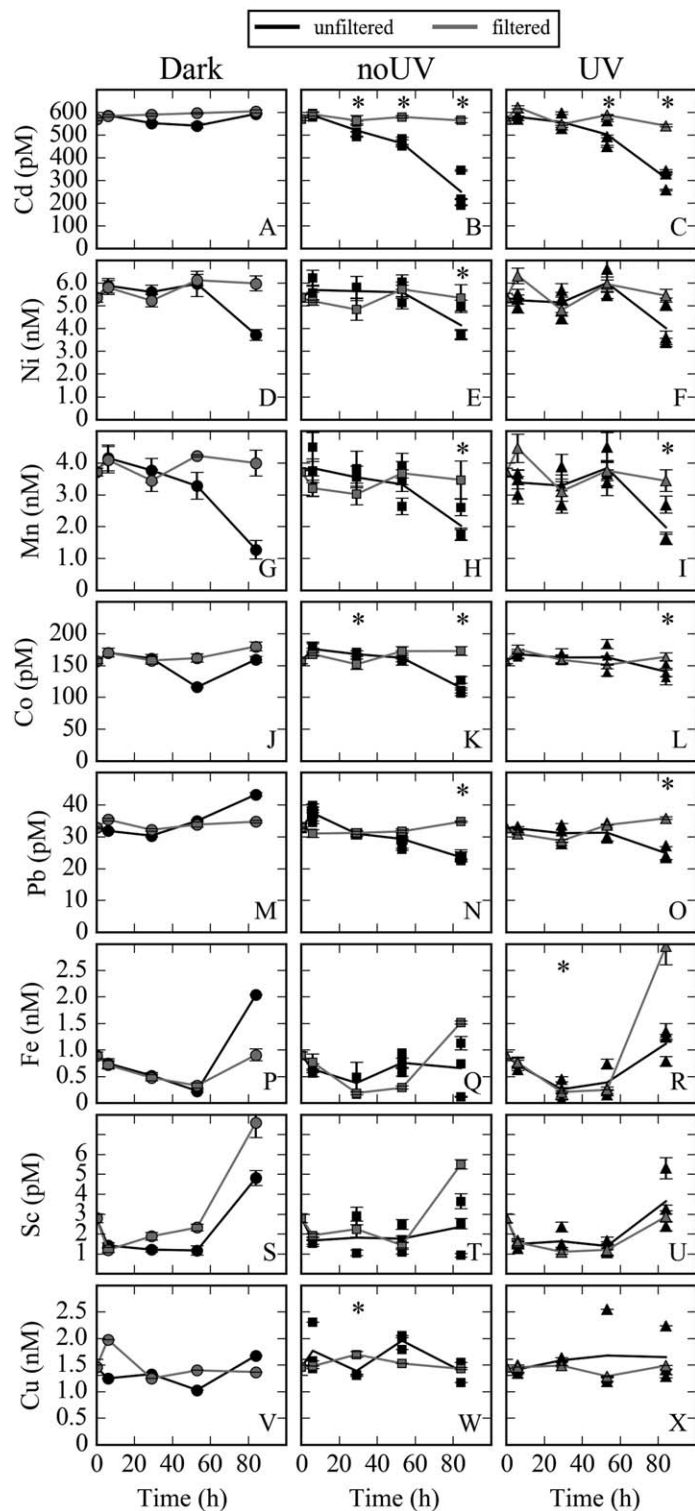
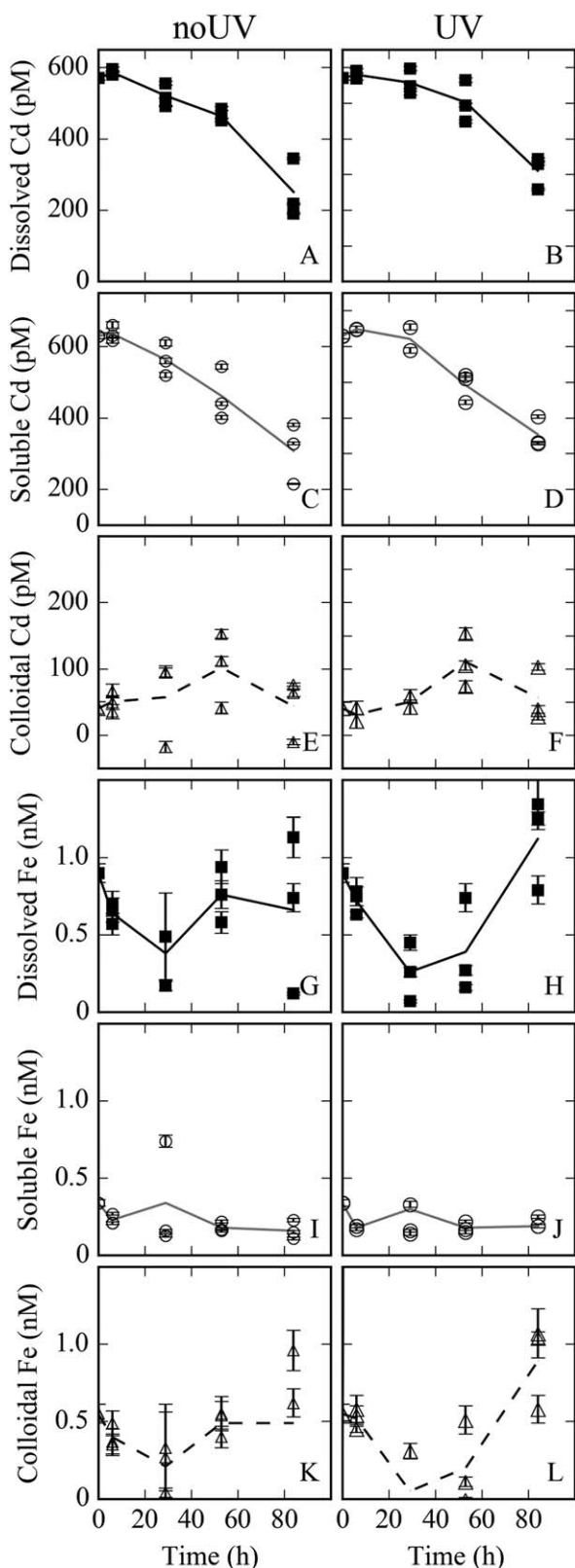


Fig. 5. see next page for caption

**Fig. 5.** Dissolved metal concentrations of filtered (< 0.2 μm; filled gray) and unfiltered (filled black) seawater for the three light treatments. Concentrations of dissolved (< 0.2 μm) (A–C) cadmium, (D–F) nickel, (G–I) manganese, (J–L) cobalt, (M–O) lead, (P–R) iron, (S–U) scandium, and (V–X) copper are presented for Dark (left), noUV (middle), and UV (right) treatments. Each data point represents a discrete replicate of the treatment time point, error bars represent the relative standard deviation of analytical measurements of each time point replicate, and the line connects the average of all results for the treatment time points. Note that no replicate time point samples exist for Dark and filtered treatments. \* results that are significantly different ( $t$ -test,  $p < 0.05$ ) from the 6-h time point.





**Fig. 6.** see next page for caption

continued increasing through the end of the incubation experiments, with final concentrations nearly double the concentrations observed in the UV<sub>filtered</sub> (Fig. 7). A similar trend was observed for total and excess Cu-binding organic ligands, which also increased slightly over the course of the incubation experiment in both the UV and noUV compared to the filtered controls (Fig. 7). In the noUV, this increase in Cu-binding ligand concentrations was small but statistically significant relative to the 6 h speciation measurements (*t*-test, *p* < 0.05) in the 53 h and 84 h samples.

**Discussion**

**Abiotic drivers of metal cycling**

*The effect of UV light and temperature on Fe uptake*

In the first 6–7 h of the experiment, there were significantly faster short-term Fe uptake rates (ANOVA, *p* < 0.05) in all size fractions of phytoplankton exposed to the UV treatment relative to those exposed to noUV (Table 2). Higher Fe uptake rates in the presence of UV light were also observed in the first measurement of the long-term uptake rates for the > 5 μm and 1–5 μm size fractions, although these differences were not statistically significant (ANOVA, *p* > 0.05; Table 2). These observations indicate that UV light increased the bioavailability of in situ Fe to all phytoplankton at the onset of the experiment. This is consistent with photochemical reductive dissociation of Fe from strong organic ligands resulting in release of highly bioavailable Fe(II) (Barbeau et al. 2001).

After the first 29 h of the experiment, Chl *a* began to increase, and the biomass-normalized long-term Fe uptake rates decreased. Excess Fe-binding ligand concentrations increased with the increase in biomass during the experiment, resulting in an inverse relationship between excess L and Fe uptake rates (Fig. 10A,B), as was described in Maldonado and Price (2001). It is not clear from these data whether slower Fe uptake rates may have stimulated ligand production, resulting in the observed increase in excess L, or whether increases in excess L as a function of community growth led to slower Fe uptake rates due to competition for Fe' between excess L and the cell surface Fe transporters

**Fig. 6.** Dissolved (“d,” < 0.2 μm, filled black squares), soluble (“s,” < 0.02 μm, open circles), and colloidal ([dM] – [sM], open triangles) for cadmium (Cd) and iron (Fe) concentrations for noUV (left) and UV (right) treatments. For each light treatment, (A, B) dissolved Cd, (C, D) soluble Cd, (E, F) colloidal Cd, (G, H) dissolved Fe, (I, J) soluble Fe, and (K, L) colloidal Fe are presented. Each data point represents a discrete replicate of the treatment time point, error bars represent the relative standard deviation of analytical measurements of each time point replicate, and the line connects the average of all results for the treatment time points. Note that colloidal cadmium and iron represents the difference between the dissolved (< 0.2 μm) and soluble (< 0.02 μm) data. Error bars represent the relative standard deviation for each sample.

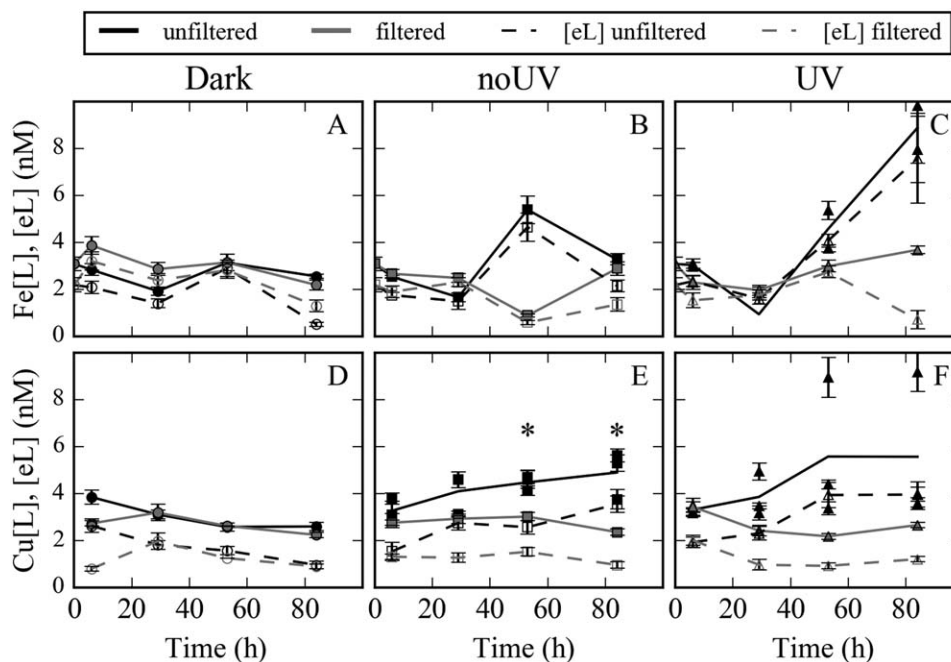


**Fig. 7.** Dissolved (< 0.2 μm) concentrations of Fe- and Cu-binding ligands (nM) for three light treatments. **(A–C)** Fe- and **(D–F)** Cu-binding ligands are presented for Dark (left), noUV (middle), and UV (right) treatments. Each subfigure displays the unfiltered (filled black) and filtered (< 0.2 μm; filled gray) ligand concentrations, and excess ligand (eL) data is included using unfilled markers and dotted lines. Each data point represents a discrete replicate of the treatment time point, error bars represent the relative standard deviation of analytical measurements of each time point replicate, and the line connects the average of all results for the treatment time points. Note that no replicate time point samples exist for Dark and filtered treatments. \* results that are significantly different (*t*-test, *p* < 0.05) from the 6-h time point.

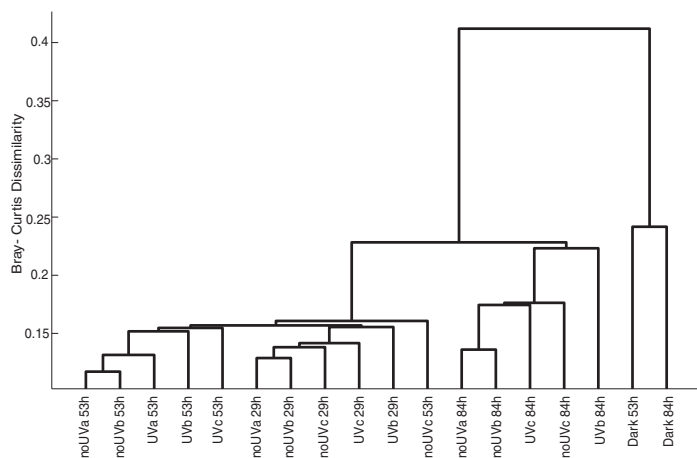


**Fig. 8.** A cluster dendrogram showing the Bray-Curtis dissimilarity of diatom 18S amplicon sequencing results from all incubation treatments sampled throughout the course of the experiment.

(Maldonado et al. 2001). Regardless, the reemergence of significantly (ANOVA, *p* < 0.05) faster Fe uptake rates for the largest size fraction (> 5 μm) in the UV during the final long-term Fe uptake measurement suggest that some of the produced ligands may have been photoreactive, leading to increased Fe bioavailability (Fig. 4D). Furthermore, Fe : C

assimilation ratios in the incubation were comparable to those observed in cultures of coastal diatoms (Sunda and Huntsman 1995b; Maldonado and Price 1996), even though [Fe'] was almost two orders of magnitude lower in our experiment, indicating that some of the FeL was likely bioavailable (Table 2).

In addition to increased excess L concentrations competing for Fe', the increase in water temperature from 12.8°C to ~ 19°C in the first 53 h of the incubation (Supporting Information Fig. S3) may have contributed to the lower Fe uptake rates observed between those time points. Sunda and Huntsman (2003) have shown the photo-reductive steady state concentration of Fe' to be twofold to threefold higher at 10°C vs. 20°C in laboratory experiments with EDTA due to the relatively unchanged rate of photo-dissociation relative to the large negative effect on Fe(II)' oxidation and chelation of Fe(III)' at lower temperatures. Similarly, Hassler et al. (2013) reported twofold greater Fe' values when conducting CLE-AdCSV measurements on natural organic ligands at 4°C vs. ~ 20°C.

**The effects of UV light on trace metal concentration and speciation**

Despite the difference in Fe uptake rates between the light treatments, dissolved and soluble Fe concentrations were indistinguishable (Fig. 5). Speciation measurements showed



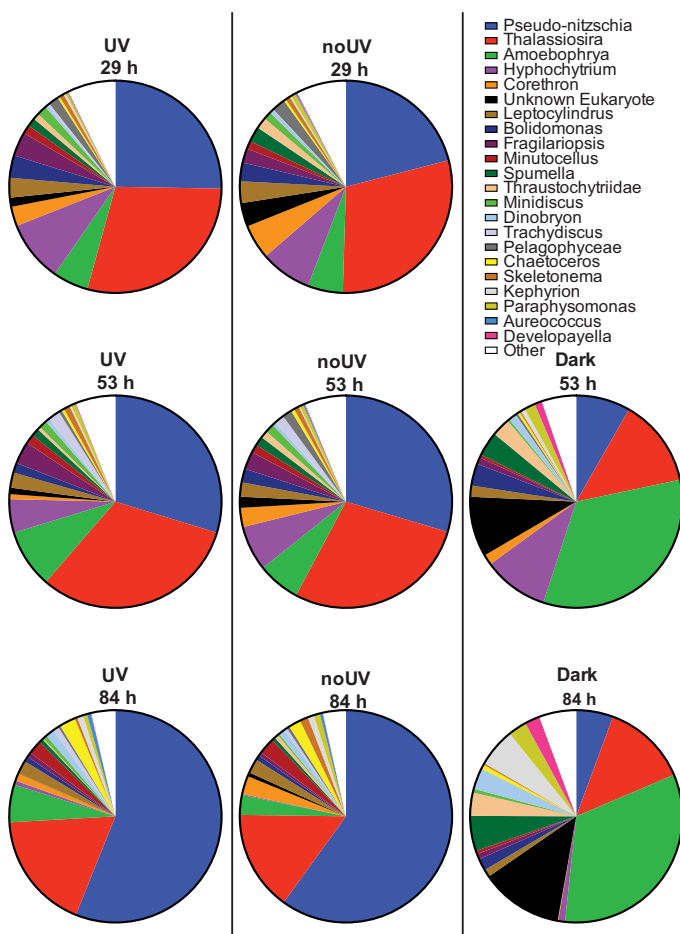


**Fig. 9.** A series of pie charts that shows the fraction of diatom 18S sequences attributed to a given genera for one representative sample of each treatment and time point during the incubation. Only the top 10 genera from each of the representative samples are named with the remaining genera grouped together in the “other” category.

Fe was complexed by strong organic ligands ( $\log K_{\text{FeL,Fe}'}^{\text{cond}} = 12.98 \pm 0.29$ ) at the start of the incubation (Table S3). Siderophores are strong Fe-binding organic ligands produced by bacteria as an Fe acquisition strategy (Sandy and Butler 2009). Previous studies of the influence of photochemistry on Fe speciation have found that some siderophores are highly photoreactive (Barbeau et al. 2002; Barbeau et al. 2003; Kupper et al. 2006; Amin et al. 2009), resulting in the reduction and release of Fe from the complex and formation of a weaker oxidized ligand. While nonphotoreactive siderophores are most commonly characterized from marine surface waters (Mawji et al. 2008; Boiteau et al. 2013), there is also genetic evidence for the production of photoreactive siderophores in natural waters that may be short-lived due to their relatively high reactivity (Gärdes et al. 2013).

Evidence of photoreactive Fe-binding ligands was observed in the short-term Fe uptake rate measurements,

where photoreduction seemed to have resulted in more of the bioavailable  $\text{Fe}'$  species in the UV than the noUV treatment (Fig. 4; Table 2). The photoreactivity of the initial ligand pool was evident in the  $\text{UV}_{\text{filtered}}$  treatment, where binding capacity ( $\alpha'_{\text{FeL}}$ ) decreased 10-fold and  $[\text{Fe}']$  increased sevenfold in the first 53 h (Table S3). Moreover, in the  $\text{noUV}_{\text{filtered}}$  and  $\text{Dark}_{\text{filtered}}$  treatments, stronger  $L_1$ -type Fe-binding organic ligands were detected throughout the incubation (Table S3). In contrast—excluding the 84 h sample that was impacted by the colloidal Fe pulse, which may have led to an overestimation of  $L_1$  (or rather of the  $K_{\text{FeL,Fe}'}^{\text{cond}}$  of  $L_i$ ) if colloidal Fe did not exchange with the added competing ligand (Gledhill and Buck 2012), see “Background effects of Cubitainers” section and “Fe- and Cu-binding ligand production” section below—only weaker  $L_2$ -type ligands with declining stability constants were observed in the  $\text{UV}_{\text{filtered}}$  treatment over the 53 h of the incubation.

The decreases in  $K_{\text{FeL,Fe}'}^{\text{cond}}$  observed in the  $\text{UV}_{\text{filtered}}$  treatment were similar to those resulting from the photodegradation of catecholate-type and mixed catecholate/ $\alpha$ -hydroxy carboxylate-type siderophores from culture extracts (Barbeau et al. 2003). Depth profiles of Fe-binding ligands measured in a recent study in the CCS also reported higher concentrations of  $L_1$  and  $L_2$  ligands below the euphotic zone of several stations (Bundy et al. 2016). Thus, our observations may suggest that a portion of the dissolved ligand pool in the recently upwelled waters used for this experiment contained photoreactive siderophores that enhanced  $\text{Fe}'$  at the onset of the incubation. Even after only 6 h, the weaker Fe complexation in the  $\text{UV}_{\text{filtered}}$  treatment resulted in  $[\text{Fe}']$  more than triple those determined in the  $\text{noUV}_{\text{filtered}}$  and  $\text{Dark}_{\text{filtered}}$  treatment samples ( $[\text{Fe}']$  of  $10^{-12.34}$  M, compared to  $10^{-12.88}$  M and  $10^{-12.97}$  M, respectively; Table S3), and lend support to the observations of higher short-term Fe uptake in the unfiltered version of this treatment.

The observations of Cu-binding ligands in the filtered light treatments showed no evidence for photochemical cycling. A single class of Cu-binding ligands was measured, and the concentrations of these ligands were mostly invariant over the course of the experiment in both  $\text{UV}_{\text{filtered}}$  and  $\text{noUV}_{\text{filtered}}$  (Fig. 7D–F). Although a slight decline in the conditional stability constants was observed in the last three samples of the  $\text{UV}_{\text{filtered}}$  treatment, it is not a significant departure from values observed in the  $\text{noUV}_{\text{filtered}}$  samples. Overall, the combined observations from the  $\text{UV}_{\text{filtered}}$  and  $\text{noUV}_{\text{filtered}}$  treatments for Fe- and Cu-binding ligands present a complex organic ligand pool in which size, functional group, and binding strength likely play a role in reactivity and metal cycling.

### Background effects of Cubitainers

It is particularly challenging in trace metal incubation experiments to distinguish between biological metal cycling, abiotic scavenging, and interactions with the containers. In

**Table 2.** Short-term Fe (pmol Fe  $\mu\text{g Chl } a^{-1} \text{ h}^{-1}$ ) and C ( $\mu\text{mol C } \mu\text{g Chl } a^{-1} \text{ h}^{-1}$ ) uptake rates, as well as calculated Fe:C assimilation ratios measured in the first 7 h of the experiment for each of the light treatments. Values represent the average  $\pm$  standard deviation of three replicate measurements for each size fraction and light treatment.

Size fraction	Fe uptake (pmol Fe $\mu\text{g Chl } a^{-1} \text{ h}^{-1}$ )			C uptake ( $\mu\text{mol C } \mu\text{g Chl } a^{-1} \text{ h}^{-1}$ )		
	0.2–1 $\mu\text{m}$	1–5 $\mu\text{m}$	> 5 $\mu\text{m}$	0.2–1 $\mu\text{m}$	1–5 $\mu\text{m}$	> 5 $\mu\text{m}$
UV	12.1 $\pm$ 1.4*	10 $\pm$ 0.6*	11 $\pm$ 0.6*	0.14 $\pm$ 0.05	0.46 $\pm$ 0.05	0.48 $\pm$ 0.13
noUV	6.7 $\pm$ 2.6	4.9 $\pm$ 2.1	4.8 $\pm$ 2.1	0.17 $\pm$ 0.02	0.51 $\pm$ 0.02	0.66 $\pm$ 0.11
Dark	3.6 $\pm$ 0.6	1.7 $\pm$ 0.2	2.1 $\pm$ 0.2	0.06 $\pm$ 0.01	0.03 $\pm$ 0.01	0.03 $\pm$ 0.01
	Fe : C ( $\mu\text{mol Fe mol C}^{-1}$ )			[Fe'] (pM)	Source	
UV	86 $\pm$ 1.4	22 $\pm$ 0.6	23 $\pm$ 0.6	0.07	This study ([Fe'] from $t = 0$ h)	
noUV	39 $\pm$ 2.6	9.6 $\pm$ 2.2	7.3 $\pm$ 2.1	0.07	This study ([Fe'] from $t = 0$ h)	
<b>Laboratory cultures<sup>‡</sup></b>						
<i>T. weissflogii</i> (Fe replete)	—	—	40 $\pm$ 0.02	40,000	Maldonado and Price (1996)	
<i>T. pseudonana</i> (Fe replete)	—	—	56 $\pm$ 0.1	40,000	Maldonado and Price (1996)	
<i>P. cf. calliantha</i> (Fe replete)	—	—	221.5 $\pm$ 26.5	1000 <sup>†</sup>	Marchetti et al. (2006)	
<i>T. pseudonana</i> (Fe limited)	—	—	14 $\pm$ 0.1	20	Maldonado and Price (1996)	
<i>T. pseudonana</i> (Fe limited)	—	—	12.5	24	Sunda and Huntsman (1995b)	
<i>T. weissflogii</i> (Fe limited)	—	—	13.1	28	Sunda and Huntsman (1995b)	
<i>T. weissflogii</i> (Fe limited)	—	—	9.73 $\pm$ 0.03	20	Maldonado and Price (1996)	
<i>P. cf. calliantha</i> (Fe limited)	—	—	10.5 $\pm$ 0.6	4 <sup>†</sup>	Marchetti et al. (2006)	
<i>P. cf. calliantha</i> (Fe limited)	—	—	5.2 $\pm$ 0.2	2 <sup>†</sup>	Marchetti et al. (2006)	

\* Points that are statistically significant (ANOVA,  $p < 0.05$ ) between UV and noUV measurements. Below, Fe : C uptake rates are calculated for each size fraction and compared to literature values observed in culture along with the [Fe'] of each study.

<sup>†</sup> Values from Marchetti et al. (2006) were originally reported as Fe<sup>3+</sup> and converted to Fe' here using the inorganic side reaction coefficient of  $10^{10}$  (Hudson et al. 1992).

<sup>‡</sup> Full names of species: *Thalassiosira weissflogii*, *Thalassiosira pseudonana*, *Pseudo-nitzschia cf. calliantha*

this experiment, filtered controls for each light treatment were used to aid in this distinction. The observed decline in dissolved Fe, Sc, and perhaps phosphate in filtered and Dark treatments, where particle scavenging and biological uptake should be absent, suggests that these elements were likely adsorbed to the walls of the container over time. Wall loss for dFe measurements has been reported in previous field (Buck et al. 2010; Fitzsimmons and Boyle 2012; King et al. 2012; Bundy et al. 2016) and laboratory experiments (Fischer et al. 2007), and this bottle adsorption has been shown to vary as a function of surface area : volume ratio of the bottle, bottle material, and temperature (Fischer et al. 2007; Fitzsimmons and Boyle 2012). Given the evidence for the chemical similarities between Fe and Sc (Rogers et al. 1980; Byrne 2002; Parker et al. 2016), it is not surprising that Sc followed similar trends as Fe in the containers. Most wall loss in the filtered treatments for Sc and soluble Fe took place within the first 6 h, while the colloidal Fe fraction declined slowly through the 29 h and 53 h time points in filtered treatments (Fig. 5). The rapid rate of wall loss of both dFe and dSc within the first 6 h of the experiment suggests that initial conditions of the incubation during the 3.5 h filling of the Cubitainers may not have been homogenous even though Cubitainers were filled from a mixed barrel. Thus, wall loss

during initial Cubitainer filling may have contributed to higher intra-treatment variability in the experiment.

The most dramatic change in dFe and dSc concentrations occurred between the final two sampling points, with the final concentrations of dFe and dSc greater than or equal to the initial concentrations in all treatments, even in unfiltered treatments where biological uptake was occurring (Fig. 5). This was also observed for dPb in the Dark, UV<sub>filtered</sub>, and noUV<sub>filtered</sub> treatments, but to a lesser magnitude than Fe or Sc (Fig. 5M–O). The observation of higher final concentrations than initial concentrations in most of the filtered treatments suggests that the source of both Fe and Sc between the last two time points was contamination from the Cubitainers themselves. This feature was not observed in the soluble Fe data, indicating that the Fe leaching from the containers was mostly colloidal Fe, or a soluble Fe input that quickly became colloidal (Hurst and Bruland 2007). This colloidal Fe did appear to be largely inorganic in nature, however, given that it generally titrated the excess Fe-binding ligands in the UV<sub>filtered</sub>, noUV<sub>filtered</sub>, and both Dark treatments (Fig. 7A–C), although the probable interpretation artifact of an inert colloidal Fe fraction as L<sub>1</sub> led to an increase in  $\alpha'_{\text{FeL}}$  (Table S3; Gledhill and Buck 2012). Previous work has shown that wall loss is an exothermic reaction (Fitzsimmons and Boyle 2012), and increases

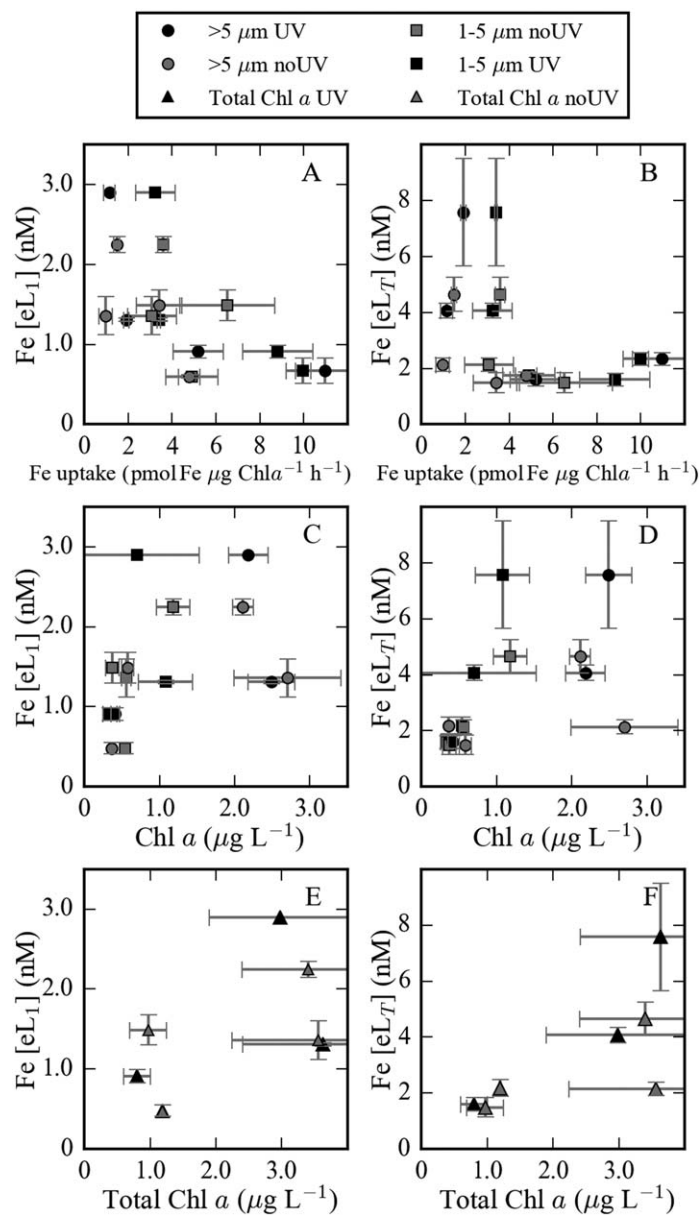


**Fig. 10.** The correlations of Fe uptake (pmol Fe μg Chl a<sup>-1</sup> h<sup>-1</sup>), Chl a concentrations (μg L<sup>-1</sup>), excess Fe L<sub>1</sub> ligands (nM), and total excess Fe ligands (nM). The top two panels display plots of (A) excess L<sub>1</sub> ligands and Fe uptake and (B) total excess Fe ligands for each size fraction a light treatment: > 5 μm UV (black circle), 1–5 μm UV (black square), > 5 μm noUV (gray circle), and 1–5 μm noUV (gray square). The middle two panels plot (C) excess Fe L<sub>1</sub> and (D) total excess Fe ligands against vs. Chl a concentrations corresponding to each size fractions mentioned above. The bottom two panels display (E) excess Fe L<sub>1</sub> and (F) total excess Fe ligands plotted against total Chl a for the UV (black triangles) and noUV (gray triangles) treatments. Error bars represent the standard deviation of each measurement.

in temperature during the incubation may have contributed to the release of Fe and Sc from the Cubitainer, though the temperature increase was confined to the first 53 h of the experiment (Supporting Information Fig. S3) and the largest

increases in Fe and Sc were observed between the 53 h and 84 h time points (Fig. 5).

In a previous experiment using a similar type of incubation container, Lohan et al. (2005) did not report any wall loss or contamination of dFe and dZn concentrations. An important distinction was that Lohan et al. (2005) employed a prolonged conditioning step for their Cubitainers, whereby each Cubitainer was filled with open-ocean seawater and left to condition for 2 d prior to the start of their incubation. This study did not employ a long conditioning step, though the Cubitainers were rinsed at least two times with filtered seawater immediately prior to filling with incubation water. Thus, it is possible that the rinses used in this experiment were not adequate to condition the walls of the containers, and a longer conditioning period may have mitigated some of the container-based effects observed.

**Biological uptake vs. abiotic scavenging of trace metals**

In this study, unfiltered treatments were used to assess the influence of ambient particles on the cycling of trace metals during the experiment as compared to filtered controls. For Cd, the dissolved and soluble Cd concentrations were relatively constant through the experiment in all filtered treatments. Only in the unfiltered light treatments (UV and noUV) did the Cd concentrations decrease appreciably (Fig. 6A,B), indicating biological uptake of Cd and especially soluble Cd. The change in Cd : P (0.36–0.47 mmol mol<sup>-1</sup>; Table 3) was similar to that observed in a previous incubation experiment with comparable initial dFe concentrations (0.41–0.44 mmol mol<sup>-1</sup>, Cullen et al. 2003). Our Cd : P ratios were also very close to P-normalized stoichiometry from the vertical profile data at Sta. 28, which reflected a Cd : P ratio of 0.3 mmol mol<sup>-1</sup> in the upper 200 m of the water column (Supporting Information Fig. S4; Table 3). Using a Redfield ratio of 106 : 1 C : P for the duration of the incubation results in Cd uptake rates of 0.97–1.27 μmol Cd mol C<sup>-1</sup> d<sup>-1</sup>, consistent with rates observed in cultures using natural waters from the North Pacific (Xu et al. 2012). This uptake of Cd in the incubation could be from nonspecific uptake through a high affinity Zn uptake system up-regulated under low Zn conditions (Sunda and Huntsman 1998), as suggested previously in the central CCS (Billler and Bruland 2013), though we do not have Zn data from our incubation experiment. Additionally, at least two species of *Thalassiosira*, a major genus in our incubation, have been observed to show a nutrient-like response to Cd additions under low Zn conditions (Price and Morel 1990; Lee and Morel 1995).

Distinct from Cd, declines in Ni and Mn concentrations during this incubation were observed in all unfiltered treatments, including in the Dark (Fig. 5D–I). Elevated initial concentrations of Mn reflected the close proximity of the incubation setup to the continental shelf break (Billler and Bruland 2013). Using Mn : P ratios for diatom species of

**Table 3.** The P normalized values for metals observed in this incubation study, at Sta. 28 near where the water was collected, and the values reported in previous studies for diatoms and profiles in the North Pacific. The values for this incubation were calculated from the drawdown of P and each metal observed over the 84 h incubation period.

Treatment/ source	Metal to P ratio (mmol mol <sup>-1</sup> )									
	Cd	Ni	Mn	Co	Pb	Fe	Sc	Cu		
UV	0.36 ± 0.08	1.84 ± 1.26	2.39 ± 0.9	0.021 ± 0.013	0.023 ± 0.015	0.70 ± 0.42*	0.002 ± 0.0003*	-0.24 ± 0.69		
noUV	0.47 ± 0.17	1.72 ± 1.05	2.41 ± 0.74	0.062 ± 0.023	0.013 ± 0.002	0.19 ± 0.27*	0.002 ± 0.0011*	0.12 ± 0.31		
Sta. 28†	0.30	0.83	-1.05	-0.002	0.021	2.2	0.003	-0.06		
Twining and Baines (2013)‡	0.07-1.29	0.21-0.68	0.33-1.7	0.15	—	5.2	—	0.18-1.44		
Cullen et al. (2005)§	0.41-0.44	—	0.66-0.70	0.09-0.1	—	—	—	0.54-0.6		
North Pacific	0.40 ± 0.11	1.0 ± 0.1	—	0.038 ± 0.002	—	0.50 ± 0.3	—	0.41 ± 0.08		

\* Values that were calculated using the 53 h measurements due to contamination observed in the 84 h samples.

† Sta. 28 P normalized metal stoichiometries from surface (15 m) to depth (200 m) measurements.

‡ Data from Twining and Banes was selected from studies that reported values from diatoms specifically.

§ Data from Cullen et al. (2003) was selected for Fe concentrations closest to those observed in the starting conditions for this study (0.5 nM and 1 nM).

|| Compiled data from Twining and Baines (2013) and references therein for P normalized stoichiometries in the upper water column (> 800 m).

0.33–1.7 mmol mol<sup>-1</sup> from Twining and Baines (2013) and a phosphate decrease in the UV and noUV treatments would predict a drawdown of 0.3–1.4 nM Mn. However, the observed decline in Mn ranged from 1.6 nM to 2.4 nM, with the largest decrease observed in the Dark. Thus, while biological uptake from diatoms was likely taking place, it cannot account for the magnitude of dMn removal observed (Fig. 5G–I). The decline in Mn across all unfiltered treatments, with greater declines in the Dark, is consistent with biotic precipitation of manganese oxides by bacteria in the experiment, which is enhanced in the dark (Lee and Fisher 1993; Francis et al. 2001; Tebo et al. 2005). Using Mn particle formation rates from Lee and Fisher (1993) under similar conditions to this incubation (1 nM Mn, 18°C) of 0.31 nM d<sup>-1</sup>, combined with the diatom Mn : P assimilation ratios above, results in a predicted decline of 1.4–2.5 nM Mn, which would account for the observed Mn decline in both the UV and noUV. Yet the rate of Mn decline observed in the Dark treatment was much faster (0.70 nM d<sup>-1</sup>) than predicted by Lee and Fisher (1993), perhaps reflecting the higher initial Mn (3.72 nM) at the onset of our experiment.

Like Mn, Ni also decreased in all unfiltered but not filtered treatments (Fig. 5D–F). Using Ni : P ratios of 0.21–0.68 mmol mol<sup>-1</sup> from Twining and Baines (2013) and the observed phosphate decline in our experiment, expected biological drawdown of Ni was 0.17–0.54 nM. The observed decrease in Ni was more than double that expected from biological uptake in the UV and noUV, ranging from 1.05 nM to 1.46 nM, and was also observed in the Dark, suggesting scavenging of Ni. This is a surprising finding for Ni, which is typically characterized by a nutrient-type profile in the North Pacific (Bruland 1980). The decline in the Dark could perhaps be from preferential scavenging of Ni on biogenic manganese oxides, which has been observed in freshwater systems (Kay et al. 2001). Alternatively, if the Mn(II) oxidation pathway is a result from extracellular production of superoxide (Learman et al. 2011), then the widespread use of Ni superoxide dismutase in bacteria (Dupont et al. 2008; Zhang and Gladyshev 2010) may have led to the observed decline in Ni as a response to increasing superoxide concentrations during Mn oxidation.

Cobalt, which has been shown to co-precipitate with manganese oxides (Lee and Fisher 1993; Moffett and Ho 1996), tracked with Mn and Ni in the UV and noUV treatments, but not through the final time point in the Dark, though only one replicate was available from each time point of this treatment (Fig. 5J–L). Using the data from just the first 53 h of the Dark results in a Co particle formation rate of 18.4 pM d<sup>-1</sup>, threefold greater than the rates observed by Lee and Fisher (1993). Alternatively, if the 53 h time point is excluded, a lack of co-variance in Co and Mn in the Dark treatment may indicate that dCo was stabilized by organic complexation (Saito and Moffett 2001; Saito et al. 2005). In this case, declines in Co in the UV and noUV



could be interpreted primarily as biological uptake of Co. The decline of Co results in Co : P ratios of 0.021–0.062 mmol mol<sup>-1</sup>, lower than those reported by Cullen et al. (2003) (0.09–0.1 mmol mol<sup>-1</sup>; Table 3). The Co : P ratios are about a order of magnitude lower than those observed in the Peru upwelling region (0.248 mmol mol<sup>-1</sup>; Saito et al. 2004), but are consistent with profile data from the North Pacific (0.038 mmol mol<sup>-1</sup>; Table 3), perhaps indicating phytoplankton in this region have lower Co quotas than those studied in the Southern Ocean or Peruvian regimes. Cyanobacteria like *Synechococcus* spp. have an obligate Co requirement, but some diatom species such as *Thalassiosira* spp., which was a dominant group in our experiment, can use Co, Cd, and Zn interchangeably for their CA (Sunda and Huntsman 1995a; Cullen and Sherrell 2005).

Dissolved Pb concentrations declined in the UV and noUV, but not in the Dark or in any of the filtered controls, suggesting a phytoplankton cell-associated mechanism of dPb removal. Unlike Co, Pb has no biological function for phytoplankton. Lead scavenging on cells has been shown to be a function of surface area : volume ratios (Fisher et al. 1987). Thus, although the majority of Chl *a* was composed of the large cells, which have low surface area : volume ratios, it is possible that an increase in total cell surface area during phytoplankton growth in the UV and noUV contributed to Pb scavenging (Fisher et al. 1987). It is also possible that some Pb was passively transported into cells (Michaels and Flegal 1990).

Of the trace metals measured in this experiment, dissolved Cu appeared the most inert, with no discernible trend in concentrations across treatments over the course of the incubation (Fig. 5V–X). Using Cu : P values appropriate for the Fe concentrations at the onset of the incubation (0.54–0.60 mmol mol<sup>-1</sup>; Cullen et al. 2003), the expected Cu drawdown ranges between 0.43 nM and 0.48 nM. Intra-treatment variability in our experiment often exceeded this range, making it challenging to discern a clear trend between treatments (Fig. 5). Biological Cu demand is associated with its role in high affinity Fe uptake systems in diatoms (Peers et al. 2005; Maldonado et al. 2006), though a Cu independent pathway for Fe acquisition in marine phytoplankton also exists (Morrissey et al. 2015). The lack of apparent decrease in Cu in our experiment may reflect rapid cycling of Cu via uptake and efflux as has been hypothesized for observations in the North Pacific (Semeniuk et al. 2016), or the inability of some diatoms to access the exceedingly low Cu<sup>2+</sup> concentrations in this experiment (Sunda and Huntsman 1995c). Indeed, despite the mosaic of phytoplankton Fe limitation occurring in the coastal North Pacific, dissolved Cu profiles here exhibit minimal changes with depth (Supporting Information Fig. S4; Biller and Bruland 2013). The absence of dCu drawdown in our incubation is also consistent with observations from previous shipboard incubation experiments (Coale 1991; Hurst and Bruland

2007; Buck et al. 2010) and field distribution studies across biological gradients (Buck and Bruland 2005; Jacquot and Moffett 2015).

Dissolved Fe, on the other hand, was among the most dynamic metals measured in the experiment. In the Dark and Dark<sub>filtered</sub> treatments Fe decline was similar, ranging from 0.57 nM to 0.67 nM over the first 29 h, indicating substantial wall loss of Fe in the Cubitainers (Fig. 6). Although Fe concentrations were clearly affected by abiotic factors (see “Background effects of Cubitainers” section above), biological activity was very likely a primary control in UV and noUV. The Fe : P ratios observed in this incubation (0.19–0.70 mmol mol<sup>-1</sup>) are far lower than those reported for suspended particles in Monterey Bay (5.2 mmol mol<sup>-1</sup>; Martin and Knauer 1973) and those observed at Sta. 28 (2.2 mmol mol<sup>-1</sup>; Table 3). They fall much closer to those observed in the North Pacific open ocean (0.50 mmol mol<sup>-1</sup>; Table 3), although it is difficult to determine the proportions of dFe decline that can be attributed to uptake given the container effects on bulk Fe concentrations measured in this study. Using the short-term Fe and C uptake rates from this experiment resulted in a calculated Fe : C uptake ratio of 22–23 μmol mol<sup>-1</sup> for phytoplankton > 1 μm in the UV treatment vs. 7.3–9.2 μmol mol<sup>-1</sup> in the noUV (Table 2). The values calculated for the noUV are consistent with those measured for Fe-limited cultured diatoms (Sunda and Huntsman 1995b; Maldonado and Price 1996; Marchetti et al. 2006). In contrast, the values calculated for the UV fall between the range for Fe limited and Fe sufficient cultures (Table 2), indicating higher Fe bioavailability in the presence of UV light in this experiment. The Fe : C uptake ratios observed in the light treatment are also consistent with the Fe : C ratios derived from the depth profile at Sta. 28 of 22 μmol mol<sup>-1</sup> assuming a Redfield ratio for C : P of 106 : 1. Our results suggest that UV light enhances Fe bioavailability and may explain enhanced Fe : C uptake in freshly upwelled waters, as previously suggested in the CCS (Biller and Bruland 2013).

Sc remains an understudied element in the ocean compared to the other metals presented here, and as far as we know this was the first attempt to track the cycling of Sc in field incubations. The existing evidence shows fundamental similarities in chemical speciation and behavior between Sc and Fe: Byrne (2002) showed similarities in inorganic speciation of the two metals, Rogers et al. (1980) reported evidence for Sc substitution in bacterial siderophores, and Parker et al. (2016) showed similar distributions and reactivity across ocean basins. The depth profile from Sta. 28 also showed very similar distributions of dFe and dSc (Supporting Information Fig. S4). In this incubation, the observed decline in dSc in the Dark<sub>filtered</sub> treatment was proportional to the decline in Fe, with ~ 50–60% presumably lost to the walls of the container (Fig. 5P). Wall loss of Sc occurred predominantly in the first 6 h, similar to soluble Fe measurements in filtered treatments. However, observations also showed a



pulse of Sc in the final sample similar to the observations of total dissolved Fe, which was an entirely colloidal Fe response. It was not possible to tell if biological uptake played significant a role in the cycling of Sc, as wall loss alone could explain the changes observed and, as with Fe, Cubitainer effects may have masked any biological signal in the dSc measurements.

### Fe- and Cu-binding ligand production

Despite the variability in dFe concentrations, Fe-binding ligand concentrations showed a clear response to phytoplankton growth, with increasing excess Fe-binding ligands associated with increasing Chl *a* in both light treatments (Figs. 7B,C, 10C,D). This increase in excess ligands in the light treatments may have been underestimated due to the addition of colloidal Fe between the last two time points that appeared to titrate excess ligands in the filtered light and both Dark treatments (Fig. 7). The addition of colloidal Fe from the Cubitainers at the end of the experiment may have led to overestimation of total [L] and  $K_{\text{FeL,Fe}'}^{\text{cond}}$  values in the 84 h time point if some of the Fe added from the Cubitainers was not exchangeable with the competitive ligand used in the CLE-AdCSV measurements (Gledhill and Buck 2012), though it is not apparent that this was the case based at least on the filtered and Dark controls (Fig. 7). Unlike total ligand concentrations, which can be biased by a kinetically inert colloidal Fe fraction, excess ligands represent the ligands actually titrated in the CLE-AdCSV measurements and are a more robust speciation result (Gledhill and Buck 2012). Thus, the increase in *excess* ligands observed in the UV and noUV treatments remains best described as ligand production associated with phytoplankton growth in our experiment.

This feature of increasing excess Fe-binding ligand concentrations concomitant with diatom growth under high nitrate : dFe ( $> 7 \mu\text{mol} : \text{nmol}$ ; King et al. 2012) ratios has now been observed in several incubation experiments (Buck et al. 2010; King et al. 2012; Bundy et al. 2016; this study). Initial nitrate : dFe in this study was  $\sim 19 \mu\text{mol} : \text{nmol}$ , and at the onset of Fe-binding ligand production, this ratio had increased to  $\sim 200 \mu\text{mol} : \text{nmol}$ . The nitrate : dFe in this study was higher than those observed in Buck et al. (2010) and King et al. (2012), and ligand production in this study was also of greater magnitude in the UV treatment than in those previous studies. It is most commonly believed that Fe ligand production is a response to Fe limited conditions (Maldonado et al. 2001; Sijerčić and Price 2015). While this study did not employ Fe amendments, another incubation using water collected near Sta. 28 showed a strong biological response to Fe additions, indicating Fe limitation of this phytoplankton community (Fitzsimmons and Chappell, unpublished data). Additionally, previous field studies have shown that nitrate : dFe values  $> 5 \mu\text{mol} : \text{nmol}$  (or dFe : nitrate  $< 0.2 \text{ nmol} : \mu\text{mol}$ ) describe Fe limitation conditions in the CCS

(Elrod et al. 2008; King and Barbeau 2011; Biller et al. 2013; Biller and Bruland 2014).

In two previous studies, ligand production was confined to the stronger ligand class (Buck et al. 2010; King et al. 2012). Here, on the other hand, Fe-binding ligand production was observed in both stronger and weaker ligand classes (Table S3). These observations are similar to those recently reported by Bundy et al. (2016) in the southern CCS, where initial nitrate : dFe levels were similar ( $\sim 20 \mu\text{mol} : \text{nmol}$ ). Using multiple analytical windows in their CLE-AdCSV measurements, which allow resolution of multiple L classes, Bundy et al. (2016) observed increases in L<sub>1</sub>, L<sub>2</sub>, and L<sub>3</sub> ligand classes in both their +Fe and +0 treatments in a 6-d field incubation. Their study, along with the observations presented here, suggest a more complex response to the Fe-ligand pool from diatom community growth than that of previous studies.

This study also observed a small increase in Cu-binding ligand concentrations concomitantly with increasing Fe-ligand concentrations in the UV and noUV (Fig. 7E,F). Previous studies by Coale (1991) and Buck et al. (2010) also examined dCu speciation during biological production in their incubation experiments, though the different analytical windows employed for Cu speciation measurements preclude direct comparison across studies (Bruland et al. 2000). The analytical window of this study was chosen to be consistent with the approach used for the recent GEOTRACES Atlantic transect (Jacquot and Moffett 2015), and the values observed here are consistent with their observations in the surface ocean ( $10^{-13}$ – $10^{-14}$  M [Cu<sup>2+</sup>]). Similar to previous incubations (Coale 1991; Buck et al. 2010), no significant change or trend was observed in [Cu<sup>2+</sup>] or  $\alpha'_{\text{CuL}}$  through this experiment (Table S4). Cu<sup>2+</sup> concentrations ( $\sim 10^{-14.2}$ – $10^{-13.3}$  M) were also below the toxicity threshold observed for phytoplankton ( $10^{-11}$  M, Brand et al. 1986), a known trigger for Cu-ligand production in previous studies (Moffett and Brand 1996).

With *Pseudo-nitzschia* spp. comprising the majority of the planktonic community by the end of the experiment (Fig. 9), it is possible that the increase in Cu-binding ligands may reflect production of domoic acid (DA), a toxin produced by *Pseudo-nitzschia* spp. that forms complexes with both Fe ( $\log K_{\text{FeDA,Fe}'}^{\text{cond}} = 8.7 \pm 0.5$ ) and Cu ( $\log K_{\text{CuDA,Cu}^{2+}}^{\text{cond}} = 9.0 \pm 0.2$ ) (Rue and Bruland 2001). While we did not measure DA in our experiment, DA concentrations approaching  $4000 \text{ pg mL}^{-1}$  ( $\sim 13 \text{ nM}$ ) were measured in incubation experiments conducted on the same cruise (Cohen et al. 2017). Due to the relatively weak  $K_{\text{CuDA,Cu}^{2+}}^{\text{cond}}$  and  $K_{\text{FeDA,Fe}'}^{\text{cond}}$  of DA, concentrations 2–3 orders of magnitude higher would be required to see sufficient changes Cu ligands in the analytical window used in this study.

Concomitant increases in weaker Fe-binding ligands ( $\log K_{\text{FeL,Fe}'}^{\text{cond}} = 11.9$ – $10.1$ ) and Cu-binding ( $\log K_{\text{CuL,Cu}^{2+}}^{\text{cond}} = 13.3$ – $14.6$ ) ligands may alternatively reflect humic-like substances or exopolymeric substances (EPS), both of which have also been

shown to bind Fe and Cu in seawater (Laglera and Van Den Berg 2009; Norman et al. 2015; Whitby and Van Den Berg 2015). The conditional stability constants measured for terrestrially derived humic substances ( $\log K_{\text{FeHS,Fe}'}^{\text{cond}} = 10.6\text{--}11.1$ ,  $\log K_{\text{CuHS,Cu}^{2+}}^{\text{cond}} = 12.0$ ; Laglera and Van Den Berg 2009) and EPS ( $\log K_{\text{FeL,Fe}'}^{\text{cond}} = 10.4\text{--}11.9$ ; Hassler et al. 2011; Hassler et al. 2015; Norman et al. 2015) allow either to be reasonable candidates for the measured Fe and Cu weaker ligands. While the conditional stability constants for EPS as a Cu binding ligand in CLE-AdCSV remain uncharacterized, the production of EPS with bacteria and algal growth (Hassler et al. 2011; Norman et al. 2015) would suggest that EPS are the best candidate for the increases in Cu ligands and weaker Fe binding ligands observed.

### Summary and conclusions

This 3-day incubation experiment was performed using water collected from the CCS to elucidate the interplay between light, phytoplankton growth, and trace metal chemistry under conditions consistent with Fe limitation of diatom communities. This study employed measurements of short- and long-term Fe uptake, total dissolved metals with colloidal fractions for Fe and Cd, Fe and Cu speciation, and phytoplankton community structure in an attempt to better understand the biogeochemical forces driving trace metal cycling in this seasonal upwelling environment.

The influence of UV light significantly increased the short-term Fe uptake rates of all size-classes of phytoplankton measured. This suggests that UV light increased the bio-availability of Fe, likely from reduction of dFe from photolabile organic complexes present at the onset of experiment. Filtered light treatments supported this interpretation of photochemical reactivity of a portion of the initial ligand pool with decreased organic complexation capacity and increased [Fe'] observed in the first 53 h of the experiment. Long-term uptake rates declined concomitantly with increases in Chl *a* and excess ligand concentrations. Increases in Fe- and Cu-binding ligands were observed in UV and noUV treatments, but were not confined to only the stronger ligand class as observed in previous experiments. The production of weaker Fe-binding ligands in addition to Cu-binding ligands could suggest overlap between the two metals and the organic ligand pool, most likely from EPS produced during diatom growth.

The cycling of Cd in this incubation was predominantly influenced by its use as a nutrient, showing significant draw-down only in the presence of light and phytoplankton. Cobalt and Pb also showed significant decreases only in the unfiltered light treatments, though to a much lesser extent than Cd, and may have resulted from Co uptake by phytoplankton and scavenging of Pb to cell surfaces. Manganese and Ni, on the other hand, exhibited similar declines across UV, noUV, and Dark treatments that were most consistent

with Mn precipitation by Mn-oxidizing bacteria and concomitant bacterial uptake or scavenging of Ni. Copper displayed no strong trends in any of the treatments used in this incubation, showing no evidence for biological uptake. The relative contributions of uptake and scavenging to Fe and Sc cycling in the experiment was difficult to determine due to a combination of wall loss at the onset of the experiment and contamination of both metals from the Cubitainers in the final time point. Incorporation of an ambient seawater equilibrium step on the order of 24–48 h prior to incubations along with the use of filtered controls to mitigate and identify these container effects is recommended for future studies.

### References

- Abualhaija, M. M., and C. M. Van Den Berg. 2014. Chemical speciation of iron in seawater using catalytic cathodic stripping voltammetry with ligand competition against salicylaldoxime. *Mar. Chem.* **164**: 60–74. doi:10.1016/j.marchem.2014.06.005
- Amin, S. A., D. H. Green, M. C. Hart, F. C. Kupper, W. G. Sunda, and C. J. Carrano. 2009. Photolysis of iron-siderophore chelates promotes bacterial-algal mutualism. *Proc. Natl. Acad. Sci. USA* **106**: 17071–17076. doi:10.1073/pnas.0905512106
- Barbeau, K. 2006. Photochemistry of organic iron (III) complexing ligands in oceanic systems. *Photochem. Photobiol.* **82**: 1505–1516. doi:10.1562/2006-06-16-IR-935
- Barbeau, K., E. L. Rue, K. W. Bruland, and A. Butler. 2001. Photochemical cycling of iron in the surface ocean mediated by microbial iron (III)-binding ligands. *Nature* **413**: 409–413. doi:10.1038/35096545
- Barbeau, K., E. L. Rue, C. G. Trick, K. W. Bruland, and A. Butler. 2003. Photochemical reactivity of siderophores produced by marine heterotrophic bacteria and cyanobacteria based on characteristic Fe (III) binding groups. *Limnol. Oceanogr.* **48**: 1069–1078. doi:10.4319/lo.2003.48.3.1069
- Barbeau, K. A., G. Zhuang, D. H. Live, and A. Butler. 2002. Petrobactin, a photoreactive siderophore produced by the oil-degrading marine bacterium *Marinobacter hydrocarbonoclasticus*. *J. Am. Chem. Soc.* **124**: 378–379. doi:10.1021/ja0119088
- Bergquist, B. A., J. Wu, and E. A. Boyle. 2007. Variability in oceanic dissolved iron is dominated by the colloidal fraction. *Geochim. Cosmochim. Acta* **71**: 2960–2974. doi:10.1016/j.gca.2007.03.013
- Billler, D. V., and K. W. Bruland. 2012. Analysis of Mn, Fe, Co, Ni, Cu, Zn, Cd, and Pb in seawater using the Nobias-chelate PA1 resin and magnetic sector inductively coupled plasma mass spectrometry (ICP-MS). *Mar. Chem.* **130–131**: 12–20. doi:10.1016/j.marchem.2011.12.001
- Billler, D. V., and K. W. Bruland. 2013. Sources and distributions of Mn, Fe, Co, Ni, Cu, Zn, and Cd relative to macronutrients along the central California coast during the spring and summer upwelling season. *Mar. Chem.* **155**: 50–70. doi:10.1016/j.marchem.2013.06.003

- Billler, D. V., T. H. Coale, R. C. Till, G. J. Smith, and K. W. Bruland. 2013. Coastal iron and nitrate distributions during the spring and summer upwelling season in the central California Current upwelling regime. *Cont. Shelf Res.* **66**: 58–72. doi:10.1016/j.csr.2013.07.003
- Billler, D. V., and K. W. Bruland. 2014. The central California Current transition zone: A broad region exhibiting evidence for iron limitation. *Prog. Oceanogr.* **120**: 370–382. doi:10.1016/j.pocean.2013.11.002
- Boiteau, R. M., J. N. Fitzsimmons, D. J. Repeta, and E. A. Boyle. 2013. Detection of iron ligands in seawater and marine cyanobacteria cultures by high-performance liquid chromatography-inductively coupled plasma-mass spectrometry. *Anal. Chem.* **85**: 4357–4362. doi:10.1021/ac3034568
- Bonnain, C., M. Breitbart, and K. N. Buck. 2016. The Ferrojan Horse Hypothesis: Iron-virus interactions in the ocean. *Front. Mar. Sci.* **3**: 82. doi:10.3389/fmars.2016.00082
- Boyd, P. W., and others. 2007. Mesoscale iron enrichment experiments 1993–2005: Synthesis and future directions. *Science* **315**: 612–617. doi:10.1126/science.1131669
- Boyd, P. W., E. Ibsanmi, S. G. Sander, K. A. Hunter, and G. A. Jackson. 2010. Remineralization of upper ocean particles: Implications for iron biogeochemistry. *Limnol. Oceanogr.* **55**: 1271. doi:10.4319/lo.2010.55.3.1271
- Brand, L. E., W. G. Sunda, and R. R. L. Guillard. 1986. Reduction of marine phytoplankton reproduction rates by copper and cadmium. *J. Exp. Mar. Biol. Ecol.* **96**: 225–250. doi:10.1016/0022-0981(86)90205-4
- Bruland, K. W. 1980. Oceanographic distributions of cadmium, zinc, nickel, and copper in the North Pacific. *Earth Planet. Sci. Lett.* **47**: 176–198. doi:10.1016/0012-821X(80)90035-7
- Bruland, K. W. 1989. Complexation of zinc by natural organic ligands in the central North Pacific. *Limnol. Oceanogr.* **34**: 269–285. doi:10.4319/lo.1989.34.2.0269
- Bruland, K. W. 1992. Complexation of cadmium by natural organic ligands in the central North Pacific. *Limnol. Oceanogr.* **37**: 1008–1017. doi:10.4319/lo.1992.37.5.1008
- Bruland, K. W., R. P. Franks, G. A. Knauer, and J. H. Martin. 1979. Sampling and analytical methods for the determination of copper, cadmium, zinc, and nickel at the nanogram per liter level in sea water. *Anal. Chim. Acta* **105**: 233–245. doi:10.1016/S0003-2670(01)83754-5
- Bruland, K. W., J. R. Donut, and D. A. Hutchins. 1991. Interactive influences of bioactive trace metals on biological production in oceanic waters. *Limnol. Oceanogr.* **36**: 1555–1577. doi:10.4319/lo.1991.36.8.1555
- Bruland, K. W., E. L. Rue, J. R. Donat, S. A. Skrabal, and J. W. Moffett. 2000. Intercomparison of voltammetric techniques to determine the chemical speciation of dissolved copper in a coastal seawater sample. *Anal. Chim. Acta* **405**: 99–113. doi:10.1016/S0003-2670(99)00675-3
- Bruland, K. W., E. L. Rue, and G. J. Smith. 2001. Iron and macronutrients in California coastal upwelling regimes: Implications for diatom blooms. *Limnol. Oceanogr.* **46**: 1661–1674. doi:10.4319/lo.2001.46.7.1661
- Bruland, K. W., E. L. Rue, G. J. Smith, and G. R. Ditullio. 2005. Iron, macronutrients and diatom blooms in the Peru upwelling regime: Brown and blue waters of Peru. *Mar. Chem.* **93**: 81–103. doi:10.1016/j.marchem.2004.06.011
- Buck, K. N., and K. W. Bruland. 2005. Copper speciation in San Francisco Bay: A novel approach using multiple analytical windows. *Mar. Chem.* **96**: 185–198. doi:10.1016/j.marchem.2005.01.001
- Buck, K. N., M. C. Lohan, C. J. Berger, and K. W. Bruland. 2007. Dissolved iron speciation in two distinct river plumes and an estuary: Implications for riverine iron supply. *Limnol. Oceanogr.* **52**: 843–855. doi:10.4319/lo.2007.52.2.0843
- Buck, K. N., K. E. Selph, and K. A. Barbeau. 2010. Iron-binding ligand production and copper speciation in an incubation experiment of Antarctic Peninsula shelf waters from the Bransfield Strait, Southern Ocean. *Mar. Chem.* **122**: 148–159. doi:10.1016/j.marchem.2010.06.002
- Buck, K. N., J. Moffett, K. A. Barbeau, R. M. Bundy, Y. Kondo, and J. Wu. 2012. The organic complexation of iron and copper: An intercomparison of competitive ligand exchange-adsorptive cathodic stripping voltammetry (CLE-ACSV) techniques. *Limnol. Oceanogr.: Methods* **10**: 496–515. doi:10.4319/lom.2012.10.496
- Buck, K. N., B. Sohst, and P. N. Sedwick. 2015. The organic complexation of dissolved iron along the US GEOTRACES (GA03) North Atlantic Section. *Deep-Sea Res. Part II Top. Stud. Oceanogr.* **116**: 152–165. doi:10.1016/j.dsr2.2014.11.016
- Bundy, R. M., M. Jiang, M. Carter, and K. A. Barbeau. 2016. Iron-binding ligands in the southern California Current System: Mechanistic studies. *Front. Mar. Sci.* **3**: 27. doi:10.3389/fmars.2016.00027
- Burnett, M. W., and C. C. Patterson. 1980. Perturbation of natural lead transport in nutrient calcium pathways of marine ecosystems by industrial lead, p. 413–438. *In* E. Goldberg, Y. Horibe, and K. Saruhashi [eds.], *Isotope marine chemistry*. Uchida Rokakuho.
- Byrne, R. H. 2002. Inorganic speciation of dissolved elements in seawater: The influence of pH on concentration ratios. *Geochem. Trans.* **2**: 11–16. doi:10.1039/b109732f
- Campos, M. L. A., and C. M. Van Den Berg. 1994. Determination of copper complexation in sea water by cathodic stripping voltammetry and ligand competition with salicylaldoxime. *Anal. Chim. Acta* **284**: 481–496. doi:10.1016/0003-2670(94)85055-0
- Capodaglio, G., K. H. Coale, and K. W. Bruland. 1990. Lead speciation in surface waters of the eastern North Pacific. *Mar. Chem.* **29**: 221–233. doi:10.1016/0304-4203(90)90015-5
- Chase, Z., P. G. Stratton, and B. Hales. 2007. Iron links river runoff and shelf width to phytoplankton biomass along the US West Coast. *Geophys. Res. Lett.* **34**: L04607. doi:10.1029/2007GL029924



- Coale, K. H. 1991. Effects of iron, manganese, copper, and zinc enrichments on productivity and biomass in the subarctic Pacific. *Limnol. Oceanogr.* **36**: 1851–1864. doi:[10.4319/lo.1991.36.8.1851](https://doi.org/10.4319/lo.1991.36.8.1851)
- Coale, K. H., and K. W. Bruland. 1988. Copper complexation in the Northeast Pacific. *Limnol. Oceanogr.* **33**: 1084–1101. doi:[10.4319/lo.1988.33.5.1084](https://doi.org/10.4319/lo.1988.33.5.1084)
- Cohen, N. R., K. A. Ellis, R. H. Lampe, H. McNair, B. S. Twining, M. T. Maldonado, M. A. Brzezinski, F. I. Kuzminov, K. Thamatrakoln, C. P. Till, K. W. Bruland, W. G. Sunda, S. Bargu, and A. Marchetti. 2017. Diatom transcriptional and physiological responses to changes in iron bioavailability across ocean provinces. *Frontiers in Marine Science* **4**: article 360.
- Cullen, J. T., Z. Chase, K. H. Coale, S. E. Fitzwater, and R. M. Sherrell. 2003. Effect of iron limitation on the cadmium to phosphorus ratio of natural phytoplankton assemblages from the Southern Ocean. *Limnol. Oceanogr.* **48**: 1079–1087. doi:[10.4319/lo.2003.48.3.1079](https://doi.org/10.4319/lo.2003.48.3.1079)
- Cullen, J. T., and R. M. Sherrell. 2005. Effects of dissolved carbon dioxide, zinc, and manganese on the cadmium to phosphorus ratio in natural phytoplankton assemblages. *Limnol. Oceanogr.* **50**: 1193–1204. doi:[10.4319/lo.2005.50.4.1193](https://doi.org/10.4319/lo.2005.50.4.1193)
- Dupont, C. L., K. Neupane, J. Shearer, and B. Palenik. 2008. Diversity, function and evolution of genes coding for putative Ni-containing superoxide dismutases. *Environ. Microbiol.* **10**: 1831–1843. doi:[10.1111/j.1462-2920.2008.01604.x](https://doi.org/10.1111/j.1462-2920.2008.01604.x)
- Dupont, C. L., K. N. Buck, B. Palenik, and K. Barbeau. 2010. Nickel utilization in phytoplankton assemblages from contrasting oceanic regimes. *Deep-Sea Res. Part I Oceanogr. Res. Pap.* **57**: 553–566. doi:[10.1016/j.dsr.2009.12.014](https://doi.org/10.1016/j.dsr.2009.12.014)
- Ellwood, M. J., and C. M. G. Van Den Berg. 2000. Zinc speciation in the northeastern Atlantic Ocean. *Mar. Chem.* **68**: 295–306. doi:[10.1016/S0304-4203\(99\)00085-7](https://doi.org/10.1016/S0304-4203(99)00085-7)
- Ellwood, M. J., and C. M. G. Van Den Berg. 2001. Determination of organic complexation of cobalt in seawater by cathodic stripping voltammetry. *Mar. Chem.* **75**: 33–47. doi:[10.1016/S0304-4203\(01\)00024-X](https://doi.org/10.1016/S0304-4203(01)00024-X)
- Elrod, V., K. Johnson, S. Fitzwater, and J. Plant. 2008. A long-term, high-resolution record of surface water iron concentrations in the upwelling-driven central California region. *J. Geophys. Res. Oceans* **113**: C11021. doi:[10.1029/2007JC004610](https://doi.org/10.1029/2007JC004610)
- Fischer, A. C., J. J. Kroon, T. G. Verburg, T. Teunissen, and H. T. Wolterbeek. 2007. On the relevance of iron adsorption to container materials in small-volume experiments on iron marine chemistry: 55Fe-aided assessment of capacity, affinity and kinetics. *Mar. Chem.* **107**: 533–546. doi:[10.1016/j.marchem.2007.08.004](https://doi.org/10.1016/j.marchem.2007.08.004)
- Fisher, N., J. L. Teyssie, S. Krishnaswami, and M. Baskaran. 1987. Accumulation of Th, Pb, U, and Ra in marine phytoplankton and its geochemical significance. *Limnol. Oceanogr.* **32**: 131–142. doi:[10.4319/lo.1987.32.1.0131](https://doi.org/10.4319/lo.1987.32.1.0131)
- Fitzsimmons, J. N., and E. A. Boyle. 2012. An intercalibration between the GEOTRACES GO-FLO and the MITESS/Vanes sampling systems for dissolved iron concentration analyses (and a closer look at adsorption effects). *Limnol. Oceanogr.: Methods* **10**: 437–450. doi:[10.4319/lom.2012.10.437](https://doi.org/10.4319/lom.2012.10.437)
- Fitzsimmons, J. N., and E. A. Boyle. 2014. Both soluble and colloidal iron phases control dissolved iron variability in the tropical North Atlantic Ocean. *Geochim. Cosmochim. Acta* **125**: 539–550. doi:[10.1016/j.gca.2013.10.032](https://doi.org/10.1016/j.gca.2013.10.032)
- Francis, C. A., E. M. Co, and B. M. Tebo. 2001. Enzymatic manganese (II) oxidation by a marine  $\alpha$ -proteobacterium. *Appl. Environ. Microbiol.* **67**: 4024–4029. doi:[10.1128/AEM.67.9.4024-4029.2001](https://doi.org/10.1128/AEM.67.9.4024-4029.2001)
- Gärdes, A., C. Triana, S. A. Amin, D. H. Green, A. Romano, L. Trimble, and C. J. Carrano. 2013. Detection of photoactive siderophore biosynthesis genes in the marine environment. *Biometals* **26**: 507–516. doi:[10.1007/s10534-013-9635-1](https://doi.org/10.1007/s10534-013-9635-1)
- Gerringa, L. J. A., M. J. A. Rijkenberg, V. Schoemann, P. Laan, and H. J. W. D. Baar. 2015. Organic complexation of iron in the West Atlantic Ocean. *Mar. Chem.* **177**: 434–446. doi:[10.1016/j.marchem.2015.04.007](https://doi.org/10.1016/j.marchem.2015.04.007)
- Gledhill, M., and C. M. Van Den Berg. 1994. Determination of complexation of iron (III) with natural organic complexing ligands in seawater using cathodic stripping voltammetry. *Mar. Chem.* **47**: 41–54. doi:[10.1016/0304-4203\(94\)90012-4](https://doi.org/10.1016/0304-4203(94)90012-4)
- Gledhill, M., and K. N. Buck. 2012. The organic complexation of iron in the marine environment: A review. *Front. Microbiol.* **3**: 69. doi:[10.3389/fmicb.2012.00069](https://doi.org/10.3389/fmicb.2012.00069)
- Hassler, C. S., E. Alasonati, C. A. M. Nichols, and V. I. Slaveykova. 2011. Exopolysaccharides produced by bacteria isolated from the pelagic Southern Ocean - role in Fe binding, chemical reactivity, and bioavailability. *Mar. Chem.* **123**: 88–98. doi:[10.1016/j.marchem.2010.10.003](https://doi.org/10.1016/j.marchem.2010.10.003)
- Hassler, C. S., F.-E. Legiret, and E. C. Butler. 2013. Measurement of iron chemical speciation in seawater at 4°C: The use of competitive ligand exchange-adsorptive cathodic stripping voltammetry. *Mar. Chem.* **149**: 63–73. doi:[10.1016/j.marchem.2012.12.007](https://doi.org/10.1016/j.marchem.2012.12.007)
- Hassler, C. S., L. Norman, C. A. M. Nichols, L. A. Clementson, C. Robinson, V. Schoemann, R. J. Watson, and M. A. Doblin. 2015. Iron associated with exopolymeric substances is highly bioavailable to oceanic phytoplankton. *Mar. Chem.* **173**: 136–147. doi:[10.1016/j.marchem.2014.10.002](https://doi.org/10.1016/j.marchem.2014.10.002)
- Holm-Hansen, O., and B. Riemann. 1978. Chlorophyll a determination: Improvements in methodology. *Oikos* **30**: 438–447. doi:[10.2307/3543338](https://doi.org/10.2307/3543338)
- Hudson, R. J., D. T. Covault, and F. M. Morel. 1992. Investigations of iron coordination and redox reactions in seawater using 59Fe radiometry and ion-pair solvent extraction of amphiphilic iron complexes. *Mar. Chem.* **38**: 209–235. doi:[10.1016/0304-4203\(92\)90035-9](https://doi.org/10.1016/0304-4203(92)90035-9)

- Hurst, M. P., and K. W. Bruland. 2007. An investigation into the exchange of iron and zinc between soluble, colloidal, and particulate size-fractions in shelf waters using low-abundance isotopes as tracers in shipboard incubation experiments. *Mar. Chem.* **103**: 211–226. doi:10.1016/j.marchem.2006.07.001
- Hutchins, D., G. Ditullio, Y. Zhang, and K. Bruland. 1998. An iron limitation mosaic in the California upwelling regime. *Limnol. Oceanogr.* **43**: 1037–1054. doi:10.4319/lo.1998.43.6.1037
- Jacquot, J. E., and J. W. Moffett. 2015. Copper distribution and speciation across the International GEOTRACES Section GA03. *Deep-Sea Res. Part II Top. Stud. Oceanogr.* **116**: 187–207. doi:10.1016/j.dsr2.2014.11.013
- Johnson, K. S., and others. 2007. Developing standards for dissolved iron in seawater. *Eos* **88**: 131–132. doi:10.1029/2007EO110003
- Kay, J. T., M. H. Conklin, C. C. Fuller, and P. A. O'Day. 2001. Processes of nickel and cobalt uptake by a manganese oxide forming sediment in Pinal Creek, Globe Mining District, Arizona. *Environ. Sci. Technol.* **35**: 4719–4725. doi:10.1021/es010514d
- King, A. L., and K. A. Barbeau. 2011. Dissolved iron and macronutrient distributions in the southern California Current System. *J. Geophys. Res. Oceans* **116**: C03018. doi:10.1029/2010JC006324
- King, A. L., K. N. Buck, and K. A. Barbeau. 2012. Quasi-Lagrangian drifter studies of iron speciation and cycling off Point Conception, California. *Mar. Chem.* **128–129**: 1–12. doi:10.1016/j.marchem.2011.11.001
- Kondo, Y., S. Takeda, J. Nishioka, H. Obata, K. Furuya, W. K. Johnson, and C. S. Wong. 2008. Organic iron (III) complexing ligands during an iron enrichment experiment in the western subarctic North Pacific. *Geophys. Res. Lett.* **35**: L12601. doi:10.1029/2008GL033354
- Kupper, F. C., C. J. Carrano, J.-U. Kuhn, and A. Butler. 2006. Photoreactivity of iron(III)-aerobactin: Photoproduct structure and iron(III) coordination. *Inorg. Chem.* **45**: 6028–6033. doi:10.1021/ic0604967
- Lagerström, M. E., M. P. Field, M. Séguret, L. Fischer, S. Hann, and R. M. Sherrell. 2013. Automated on-line flow-injection ICP-MS determination of trace metals (Mn, Fe, Co, Ni, Cu and Zn) in open ocean seawater: Application to the GEOTRACES program. *Mar. Chem.* **155**: 71–80. doi:10.1016/j.marchem.2013.06.001
- Laglera, L. M., and C. M. Van Den Berg. 2009. Evidence for geochemical control of iron by humic substances in seawater. *Limnol. Oceanogr.* **54**: 610–619. doi:10.4319/lo.2009.54.2.0610
- Lane, T. W., and F. M. M. Morel. 2000. A biological function for cadmium in marine diatoms. *Proc. Natl. Acad. Sci. USA* **97**: 4627–4631. doi:10.1073/pnas.090091397
- Learman, D., B. Voelker, A. Vazquez-Rodriguez, and C. Hansel. 2011. Formation of manganese oxides by bacterially generated superoxide. *Nat. Geosci.* **4**: 95. doi:10.1038/ngeo1055
- Lee, B. G., and N. S. Fisher. 1993. Microbially mediated cobalt oxidation in seawater revealed by radiotracer experiments. *Limnol. Oceanogr.* **38**: 1593–1602. doi:10.4319/lo.1993.38.8.1593
- Lee, J. G., and F. M. Morel. 1995. Replacement of zinc by cadmium in marine phytoplankton. *Mar. Ecol. Prog. Ser.* **127**: 305–309. doi:10.3354/meps127305
- Lis, H., C. Kranzler, N. Keren, and Y. Shaked. 2015. A comparative study of iron uptake rates and mechanisms amongst marine and fresh water cyanobacteria: Prevalence of reductive iron uptake. *Life* **5**: 841–860. doi:10.3390/life5010841
- Liu, X., and F. J. Millero. 2002. The solubility of iron in seawater. *Mar. Chem.* **77**: 43–54. doi:10.1016/S0304-4203(01)00074-3
- Lohan, M. C., D. W. Crawford, D. A. Purdie, and P. J. Statham. 2005. Iron and zinc enrichments in the north-eastern subarctic Pacific: Ligand production and zinc availability in response to phytoplankton growth. *Limnol. Oceanogr.* **50**: 1427. doi:10.4319/lo.2005.50.5.1427
- Maldonado, M., and N. Price. 1996. Influence of N substrate on Fe requirements of marine centric diatoms. *Mar. Ecol. Prog. Ser.* **141**: 161–172. doi:10.3354/meps141161
- Maldonado, M. T., and N. M. Price. 1999. Utilization of iron bound to strong organic ligands by plankton communities in the subarctic Pacific Ocean. *Deep-Sea Res. Part II Top. Stud. Oceanogr.* **46**: 2447–2473. doi:10.1016/S0967-0645(99)00071-5
- Maldonado, M. T., and N. M. Price. 2001. Reduction and transport of organically bound iron by *Thalassiosira oceanica* (Bacillariophyceae). *J. Phycol.* **37**: 298–310. doi:10.1046/j.1529-8817.2001.037002298.x
- Maldonado, M. T., and others. 2001. Iron uptake and physiological response of phytoplankton during a mesoscale Southern Ocean iron enrichment. *Limnol. Oceanogr.* **46**: 1802–1808. doi:10.4319/lo.2001.46.7.1802
- Maldonado, M. T., A. E. Allen, J. S. Chong, K. Lin, D. Leus, N. Karpenko, and S. L. Harris. 2006. Copper-dependent iron transport in coastal and oceanic diatoms. *Limnol. Oceanogr.* **51**: 1729–1743. doi:10.4319/lo.2006.51.4.1729
- Marchetti, A., M. T. Maldonado, E. S. Lane, and P. J. Harrison. 2006. Iron requirements of the pennate diatom *Pseudonitzschia*: Comparison of oceanic (high-nitrate, low-chlorophyll waters) and coastal species. *Limnol. Oceanogr.* **51**: 2092–2101. doi:10.4319/lo.2006.51.5.2092
- Martin, J. H., and G. A. Knauer. 1973. The elemental composition of plankton. *Geochim. Cosmochim. Acta* **37**: 1639–1653. doi:10.1016/0016-7037(73)90154-3
- Martin, J. H., and S. E. Fitzwater. 1988. Iron deficiency limits phytoplankton growth in the north-east Pacific subarctic. *Nature* **331**: 947–975. doi:10.1038/331341a0
- Mawji, E., and others. 2008. Hydroxamate siderophores: Occurrence and importance in the Atlantic Ocean. *Environ. Sci. Technol.* **42**: 8675–8680. doi:10.1021/es801884r
- Michaels, A. F., and A. R. Flegal. 1990. Lead in marine planktonic organisms and pelagic food webs. *Limnol. Oceanogr.* **35**: 287–295. doi:10.4319/lo.1990.35.2.0287



- Moffett, J. W., and L. E. Brand. 1996. Production of strong, extracellular Cu chelators by marine cyanobacteria in response to Cu stress. *Limnol. Oceanogr.* **41**: 388–395. doi:10.4319/lo.1996.41.3.0388
- Moffett, J. W., and J. Ho. 1996. Oxidation of cobalt and manganese in seawater via a common microbially catalyzed pathway. *Geochim. Cosmochim. Acta* **60**: 3415–3424. doi:10.1016/0016-7037(96)00176-7
- Moffett, J. W., and C. Dupont. 2007. Cu complexation by organic ligands in the sub-arctic NW Pacific and Bering Sea. *Deep-Sea Res. Part I Oceanogr. Res. Pap.* **54**: 586–595. doi:10.1016/j.dsr.2006.12.013
- Moore, J. K., S. C. Doney, and K. Lindsay. 2004. Upper ocean ecosystem dynamics and iron cycling in a global three-dimensional model. *Global Biogeochem. Cycles* **18**: GB4028. doi:10.1029/2004GB002220
- Morel, F. M. M., and N. M. Price. 2003. The biogeochemical cycles of trace metals in the oceans. *Science* **300**: 944–947. doi:10.1126/science.1083545
- Morel, F. M. M., A. B. Kustka, and Y. Shaked. 2008. The role of unchelated Fe in the iron limitation of phytoplankton. *Limnol. Oceanogr.* **53**: 400–404. doi:10.2307/40006180
- Morrissey, J., and others. 2015. A novel protein, ubiquitous in marine phytoplankton, concentrates iron at the cell surface and facilitates uptake. *Curr. Biol.* **25**: 364–371. doi:10.1016/j.cub.2014.12.004
- Nimmo, M., C. M. G. Van Den Berg, and J. Brown. 1989. The chemical speciation of dissolved nickel, copper, vanadium and iron in Liverpool Bay, Irish Sea. *Estuar. Coast. Shelf Sci.* **29**: 57–74. doi:10.1016/0272-7714(89)90073-5
- Norman, L., and others. 2015. The role of bacterial and algal exopolymeric substances in iron chemistry. *Mar. Chem.* **173**: 148–161. doi:10.1016/j.marchem.2015.03.015
- Oldham, V. E., S. M. Owings, M. R. Jones, B. M. Tebo, and G. W. Luther. 2015. Evidence for the presence of strong Mn (III)-binding ligands in the water column of the Chesapeake Bay. *Mar. Chem.* **171**: 58–66. doi:10.1016/j.marchem.2015.02.008
- Omanović, D., C. Garnier, and I. Pižeta. 2015. ProMCC: An all-in-one tool for trace metal complexation studies. *Mar. Chem.* **173**: 25–39. doi:10.1016/j.marchem.2014.10.011
- Parker, C. E., M. T. Brown, and K. W. Bruland. 2016. Scandium in the open ocean: A comparison with other group 3 trivalent metals. *Geophys. Res. Lett.* **43**: 2758–2764. doi:10.1002/2016GL067827
- Parsons, T. R. 1984. A manual of chemical & biological methods for seawater analysis. Pergamon Press.
- Peers, G., S.-A. Quesnel, and N. M. Price. 2005. Copper requirements for iron acquisition and growth of coastal and oceanic diatoms. *Limnol. Oceanogr.* **50**: 1149–1158. doi:10.4319/lo.2005.50.4.1149
- Pižeta, I., and others. 2015. Interpretation of complexometric titration data: An intercomparison of methods for estimating models of trace metal complexation by natural organic ligands. *Mar. Chem.* **173**: 3–24. doi:10.1016/j.marchem.2015.03.006
- Poorvin, L., S. G. Sander, I. Velasquez, E. Ibsanmi, G. R. Leclair, and S. W. Wilhelm. 2011. A comparison of Fe bio-availability and binding of a catecholate siderophore with virus-mediated lysates from the marine bacterium *Vibrio alginolyticus* PWH3a. *J. Exp. Mar. Biol. Ecol.* **399**: 43–47. doi:10.1016/j.jembe.2011.01.016
- Powell, R. T., and A. Wilson-Finelli. 2003. Photochemical degradation of organic iron complexing ligands in seawater. *Aquat. Sci.* **65**: 367–374. doi:10.1007/s00027-003-0679-0
- Price, N., and F. Morel. 1990. Cadmium and cobalt substitution for zinc in a marine diatom. *Nature* **344**: 658. doi:10.1038/344658a0
- Price, N. M., and F. M. M. Morel. 1991. Colimitation of phytoplankton growth by nickel and nitrogen. *Limnol. Oceanogr.* **36**: 1071–1077. doi:10.4319/lo.1991.36.6.1071
- Rijkenberg, M. J., L. J. Gerringa, I. Velzeboer, K. R. Timmermans, A. G. Buma, and H. J. de Baar. 2006. Iron-binding ligands in Dutch estuaries are not affected by UV induced photochemical degradation. *Mar. Chem.* **100**: 11–23. doi:10.1016/j.marchem.2005.10.005
- Rogers, H. J., C. Synge, and V. E. Woods. 1980. Antibacterial effect of scandium and indium complexes of enterochelin on *Klebsiella pneumoniae*. *Antimicrob. Agents Chemother.* **18**: 63–68. doi:10.1128/AAC.18.1.63
- Rue, E., and K. Bruland. 2001. Domoic acid binds iron and copper: A possible role for the toxin produced by the marine diatom *Pseudo-nitzschia*. *Mar. Chem.* **76**: 127–134. doi:10.1016/S0304-4203(01)00053-6
- Rue, E. L., and K. W. Bruland. 1995. Complexation of iron (III) by natural organic ligands in the Central North Pacific as determined by a new competitive ligand equilibration/adsorptive cathodic stripping voltammetric method. *Mar. Chem.* **50**: 117–138. doi:10.1016/0304-4203(95)00031-L
- Rue, E. L., and K. W. Bruland. 1997. The role of organic complexation on ambient iron chemistry in the equatorial Pacific Ocean and the response of a mesoscale iron addition experiment. *Limnol. Oceanogr.* **42**: 901–910. doi:10.4319/lo.1997.42.5.0901
- Saito, M. A., and J. W. Moffett. 2001. Complexation of cobalt by natural organic ligands in the Sargasso Sea as determined by a new high-sensitivity electrochemical cobalt speciation method suitable for open ocean work. *Mar. Chem.* **75**: 49–68. doi:10.1016/S0304-4203(01)00025-1
- Saito, M. A., J. W. Moffett, S. W. Chisholm, and J. B. Waterbury. 2002. Cobalt limitation and uptake in *Prochlorococcus*. *Limnol. Oceanogr.* **47**: 1629–1636. doi:10.4319/lo.2002.47.6.1629
- Saito, M. A., J. W. Moffett, and G. R. Ditullio. 2004. Cobalt and nickel in the Peru upwelling region: A major flux of labile cobalt utilized as a micronutrient. *Global Biogeochem. Cycles* **18**: GB4030. doi:10.1029/2003GB002216

- Saito, M. A., G. Rocap, and J. W. Moffett. 2005. Production of cobalt binding ligands in a *Synechococcus* feature at the Costa Rica upwelling dome. *Limnol. Oceanogr.* **50**: 279–290. doi:10.4319/lo.2005.50.1.0279
- Saito, M. A., T. J. Goepfert, and J. T. Ritt. 2008. Some thoughts on the concept of colimitation: Three definitions and the importance of bioavailability. *Limnol. Oceanogr.* **53**: 276–290. doi:10.4319/lo.2008.53.1.0276
- Sandy, M., and A. Butler. 2009. Microbial iron acquisition: Marine and terrestrial siderophores. *Chem. Rev.* **109**: 4580–4595. doi:10.1021/cr9002787
- Semeniuk, D. M., R. M. Bundy, A. M. Posacka, M. Robert, K. A. Barbeau, and M. T. Maldonado. 2016. Using  $^{67}\text{Cu}$  to study the biogeochemical cycling of copper in the North-east Subarctic Pacific Ocean. *Front. Mar. Sci.* **3**: 78. doi:10.3389/fmars.2016.00078
- Sijerčić, A., and N. M. Price. 2015. Hydroxamate siderophore secretion by *Pseudoalteromonas haloplanktis* during steady-state and transient growth under iron limitation. *Mar. Ecol. Prog. Ser.* **531**: 105–120. doi:10.3354/meps11338
- Sunda, W. G. 1989. Trace metal interactions with marine phytoplankton. *Biol. Oceanogr.* **6**: 411–442. doi:10.1080/01965581.1988.10749543
- Sunda, W. G., and S. A. Huntsman. 1995a. Cobalt and zinc interreplacement in marine phytoplankton: Biological and geochemical implications. *Limnol. Oceanogr.* **40**: 1404–1417. doi:10.4319/lo.1995.40.8.1404
- Sunda, W. G., and S. A. Huntsman. 1995b. Iron uptake and growth limitation in oceanic and coastal phytoplankton. *Mar. Chem.* **50**: 189–206. doi:10.1016/0304-4203(95)00035-P
- Sunda, W. G., and S. A. Huntsman. 1995c. Regulation of copper concentration in the oceanic nutricline by phytoplankton uptake and regeneration cycles. *Limnol. Oceanogr.* **40**: 132–137. doi:10.4319/lo.1995.40.1.0132
- Sunda, W. G., and S. A. Huntsman. 1996. Antagonisms between cadmium and zinc toxicity and manganese limitation in a coastal diatom. *Limnol. Oceanogr.* **41**: 373–387. doi:10.4319/lo.1996.41.3.0373
- Sunda, W. G., and S. A. Huntsman. 1998. Control of Cd concentrations in a coastal diatom by interactions among free ionic Cd, Zn, and Mn in seawater. *Environ. Sci. Technol.* **32**: 2961–2968. doi:10.1021/es980271y
- Sunda, W. G., and S. A. Huntsman. 2003. Effect of pH, light, and temperature on Fe-EDTA chelation and Fe hydrolysis in seawater. *Mar. Chem.* **84**: 35–47.
- Tagliabue, A., A. R. Bowie, P. W. Boyd, K. N. Buck, K. S. Johnson, and M. A. Saito. 2017. The integral role of iron in ocean biogeochemistry. *Nature* **543**: 51–59. doi:10.1038/nature21058
- Tebo, B. M., H. A. Johnson, J. K. McCarthy, and A. S. Templeton. 2005. Geomicrobiology of manganese (II) oxidation. *Trends Microbiol.* **13**: 421–428. doi:10.1016/j.tim.2005.07.009
- Twining, B. S., and S. B. Baines. 2013. The trace metal composition of marine phytoplankton. *Ann. Rev. Mar. Sci.* **5**: 191–215. doi:10.1146/annurev-marine-121211-172322
- Whitby, H., and C. M. Van Den Berg. 2015. Evidence for copper-binding humic substances in seawater. *Mar. Chem.* **173**: 282–290. doi:10.1016/j.marchem.2014.09.011
- Wu, J., and G. W. Luther. 1995. Complexation of Fe (III) by natural organic ligands in the Northwest Atlantic Ocean by a competitive ligand equilibration method and a kinetic approach. *Mar. Chem.* **50**: 159–177. doi:10.1016/0304-4203(95)00033-N
- Xu, Y., D. Shi, L. Aristilde, and F. M. Morel. 2012. The effect of pH on the uptake of zinc and cadmium in marine phytoplankton: Possible role of weak complexes. *Limnol. Oceanogr.* **57**: 293. doi:10.4319/lo.2012.57.1.0293
- Xu, Y., and F. M. Morel. 2013. Cadmium in marine phytoplankton, p. 509–528. *In* A. Sigel, H. Sigel, and R. K. O. Sigel [eds.], *Cadmium: From toxicity to essentiality*. Springer.
- Zhang, Y., and V. N. Gladyshev. 2010. General trends in trace element utilization revealed by comparative genomic analyses of Co, Cu, Mo, Ni, and Se. *J. Biol. Chem.* **285**: 3393–3405. doi:10.1074/jbc.M109.071746
- Zimmermann, J., R. Jahn, and B. Gemeinholzer. 2011. Barcoding diatoms: Evaluation of the V4 subregion on the 18S rRNA gene, including new primers and protocols. *Org. Divers. Evol.* **11**: 173–192. doi:10.1007/s13127-011-0050-6

#### Acknowledgments

The authors thank Ken Bruland, chief scientist of the IrnBru cruise, and the captain and crew of the R/V *Melville*. We also thank Tyler Coale, who conducted the nutrient analyses for this incubation, Rob Franks for his assistance in running and maintaining the ICP-MS at the University of California Santa Cruz Institute of Marine Science, Jacob Lustig-Yaeger for his assistance with Python code used for figures, and the two anonymous reviewers whose comments significantly improved this manuscript. KNB and TM were supported by the National Science Foundation (NSF), grant OCE-1446327. JNF was supported by a Department of Marine and Coastal Sciences postdoc fellowship at Rutgers University. MTM and CD were supported by the National Natural Sciences and Engineering Research Council of Canada (NSERC). CPT was supported by National Science Foundation grant OCE-1259776 to K. Bruland. PDC was supported by Virginia Space Grant's New Investigator Program and NSF OCE-1524482.

#### Conflict of Interest

None declared.

Submitted 15 March 2017

Revised 04 August 2017

Accepted 17 October 2017

Associate editor: James Moffett